MODELING AND SIMULATION OF SPR BIOSENSORS FOR DETECTION OF HEMOGLOBIN, ELECTROLYTES, GLUCOSE, AND MOSQUITO-BORNE INFECTIONS IN BLOOD.

By

Nishat Tasnim
20161001

A thesis submitted to the Department of Electrical and Electronic Engineering in partial fulfillment of the requirements for the degree of
M.Sc Electrical and Electronic Engineering.

Electrical and Electronic Engineering
BRAC University
September 2025

Declaration

It is hereby declared that

1. The thesis submitted is my own original work while completing master degree at BRAC University.
2. The thesis does not contain material previously published or written by a third party, except where this is appropriately cited through full and accurate referencing.
3. The thesis does not contain material which has been accepted, or submitted, for any other degree or diploma at a university or other institution.
4. I have acknowledged all main sources of help.
5. I would like to request the embargo of my thesis for 12M from the submission date due to 17.09.2025.

Student's Full Name & Signature:

Nishat Tasnim

20161001

Approval

The thesis/project titled **"Modeling and Simulation of SPR Biosensors for Detection of Hemoglobin, Electrolytes, Glucose, and Mosquito-Borne Infections in Blood."** submitted by

1. Nishat Tasnim (20161001)

of Summer, 2025 has been accepted as satisfactory in partial fulfillment of the requirement for the degree of M.Sc. in Electrical and Electronics Engineering on [20-07-2025].

Examining Committee:

Supervisor:
(Chair of the committee)

____

Dr. Abu S. M. Mohsin
Associate Professor
Department of Electrical and Electronic Engineering,
BRAC UNIVERSITY

Internal Examiner:
(Member)

____

Dr. Md. Belal Hossain Bhuian
Associate Professor
Department of Electrical and Electronic Engineering
BRAC UNIVERSITY

External Expert Examiner:
(Member)

____

Dr. Rakibul Hasan Sagor
Professor
Department of Electrical and Electronic Engineering
Islamic University of Technology (IUT), Gazipur

Chairperson (Departmental Head):

____

Dr. Md. Mosaddequr Rahman
Professor and Chairperson
Department of Electrical and Electronic Engineering
BRAC UNIVERSITY

Ethics Statement

This research was conducted in accordance with the ethical standards outlined by my academic institution. Throughout the study, utmost importance was given to integrity, honesty, and respect for intellectual property.

I acknowledge the findings of this study was previously published in the Heliyon Journal, titled **"Nanohole array integrated silver nanoparticle based dual mode sensor for Hemoglobin (Hb) detection in blood"**, https://doi.org/10.1016/j.heliyon.2024.e33445

and in Physica Scripta **"Tunable MIM-grating based SPR biosensor using metal-bismuth selenide (Bi_2Se_3)-silicon nitride (Si_3N_4) for dengue, malaria, glucose, and electrolyte detection with enhanced sensitivity."**,https://iopscience.iop.org/article/10.1088/1402-4896/adedd0 which provided foundational insights relevant to this thesis. Proper citations have been provided to give appropriate credit to the original work and to maintain academic integrity. Other outcomes of this are under review in another journal.

In preparing this thesis, I have ensured that the similarity index does not exceed 30%, without self-plagiarism is 1% and a self-plagiarism rate of approximately 58% in total 59%. These measures align with institutional standards for originality and proper citation. Any reused content from my previous works has been clearly indicated, and all sources have been appropriately referenced.

I recognize the importance of originality and intellectual honesty in research. Any form of misconduct, including plagiarism, falsification, or misrepresentation, is strictly condemned. I have taken measures to ensure the originality of this work, including utilizing plagiarism detection tools and citing all sources.

Finally, I am committed to responsible research conduct and acknowledge my ethical responsibility towards the academic community, participants, and society. I aim to contribute meaningful and ethically sound knowledge through this thesis.

Abstract

Recently, Surface Plasmon Resonance (SPR) has become an important technique in the development of sensors, surpassing traditional methods. This advancement represents an exciting frontier in nanotechnology, providing innovative solutions for the detection of biomolecules. This research is dedicated to design a simple device to measure hemoglobin (Hb) concentration in blood, detecting mosquito-borne diseases, and assessing glucose and electrolyte levels. Hemoglobin, a vital protein within red blood cells, plays a crucial role in oxygen transportation throughout the body. The device a nanohole array integrated dual-mode SPR sensor accurately measure hemoglobin concentrations, which aids to detect hemoglobin disorder. The study also explored the detection of the dengue NS1 antigen and malaria virus in humans through a MIM based grating-SPR sensor which is capable to focuses on the early identification of these mosquito-borne diseases. Additionally, glucose and electrolytes level in blood is also detected. The study simulated refractive indices of blood samples and assessed the plasmonic response through a wavelength range of 450 nm to 2500 nm. The proposed 3-layers biosensor has a top grating layer placed on a plasmonic metal base of Gold (Au) and Silver (Ag), all supported by a substrate. The plasmonic response is investigated through numerical simulation performed in ANSYS Lumerical FDTD solution 8.19.1584 for x64 version. Several key performance parameters namely Sensitivity, Full-Width-at-Half-Maximum (FWHM), Quality Factor, and Detection Accuracy were calculated to evaluate the performance of the plasmonic sensor model in biomolecular detection. The obtained results were compared with those reported in the existing literature to determine the degree of improvement and the extent of innovation introduced. It was found that the proposed design is capable of sensing the refractive indices of biomarkers across a broad wavelength range, thereby offering significant potential for advancing bio-sensing technologies.

Keywords: SPR biosensor, Silver (Ag), Gold (Au), Hemoglobin, Dengue, Malaria, Glucose, Electrolytes and Sensitivity.

Dedication

My dissertation is dedicated to my parents, friends and my supervisor.

Acknowledgement

I am deeply grateful to Allah SWT for His blessings, guidance, and grace in completing this thesis. I would like to express my gratitude to my supervisor, Dr. A. S. M. Mohsin, Associate Professor, Department of Electrical and Electronic Engineering, for his enormous recommendations, guidance and assistance throughout the process. I would also like to thank the outstanding academics and the staff of the Department of Electrical and Electronic Engineering at BRAC UNIVERSITY for their long-standing assistance and collaboration.

In addition, I would like to take this occasion to express my gratitude to everyone who has helped me succeed at BRAC UNIVERSITY.

List of Publications

I. **Nishat Tasnim[a],** and Abu S. M. Mohsin[a*] **"N. Tasnim and A. S. Mohsin, "Nanohole array integrated metal insulator metal (MIM) based structure employing dual mode SPR sensor for detection of Hemoglobin (Hb) in blood,"** ***Heliyon*****, vol. 10, no. 12, p. e33445, Jun. 2024."** (Q1,IF4.0,Citescore 4.5), https://doi.org/10.1016/j.heliyon.2024.e33445

II. **Nishat Tasnim,** and Abu S. M. Mohsin, **"N. Tasnim and A. S. Mohsin, "Tunable MIM-grating based SPR biosensor using metal-bismuth selenide (Bi_2Se_3)-silicon nitride (Si_3N_4) for dengue, malaria, glucose, and electrolyte detection with enhanced sensitivity,"** ***Phys. Scr.*****, vol. 100, no. 7, p. 075570, Jul. 2025."**, Physica Scripta (citescore 3.7, IF 2.6) https://iopscience.iop.org/article/10.1088/1402-4896/adedd0

Table of Contents

List of Tables

List of Figures

List of Acronyms

PCF	Photonic crystal fiber
MIM	Metal insulator metal
SPR	Surface plasmon resonance
SPP	Surface plasmon polaritons
Au	Gold
Ag	Silver
Ti	Titanium
PMMA	polymethylmethacrylate
NIL	Nanoimprint lithography

Chapter 1

Introduction

1.1 Background

In biochemical and medical diagnostics SPR surface plasmon resonance is widely used because of its ability to detect changes in refractive index at the interface between metal and dielectric medium. This enables label free detection of biomolecules and quantification of concentration [1].

When a polarized light beam strikes the metallic surface which is made up of plasmonic materials, the electrons at that metal dielectric interface resonate at a specific angle [1]. This makes SPR an effective sensing method, as the resonance is highly sensitive to surface changes. As we know, each analyte has a different refractive index so when the light beam with a certain frequency strikes it resonates at that certain frequency and shows a resonance peak. Researchers investigate biomolecular binding kinetics in applications including drug development, environmental monitoring, and biomarker detection by using SPR sensors, which provide real-time, label-free molecular interaction detection [2]. SPR's label-free characteristics make it particularly appealing for identifying analyte concentrations at low levels in intricate biological materials [3]. One of the key advantages of label-free detection is its ability to preserve the biological integrity of molecules, as it eliminates the need for tagging analytes with fluorescent or radioactive markers. This is particularly important for studies requiring the observation of biomolecules in their natural state. Surface Plasmon Resonance (SPR) is especially beneficial in this context, as it facilitates real-time monitoring of molecular interactions, enabling detailed analysis of binding kinetics such as association and dissociation rates—an essential feature for investigating complex biological processes [4]. Moreover, SPR offers exceptional sensitivity; it has the capability of detecting extremely low analyte concentrations, down to the picomolar range, by measuring subtle alteration in the refractive index at the sensor surface [5].

Depending on the specific application, SPR can be stimulated through various methods, including prism coupling, waveguide coupling, and grating coupling [6]. The operations of biosensors depend on three detection modes including i. angular scanning SPR ii. wavelength scanning SPR and iii. frequency domain optical SPR. The system architecture includes different types of sensors that use Fiber optic SPR sensors, chip based SPR sensors and nano structured SPR sensors. The biosensors categories depend on two factors which are analyte type that includes label free SPR biosensors and target specific SPR biosensors.

Surface Plasmon Resonance (SPR) is widely applied in various fields due to its sensitivity and label-free detection. In bio-sensing, it is used to study molecular interactions, such as antigen-antibody and protein-protein binding [2]. It also plays a key role in drug discovery by screening drug candidates through binding analysis with target molecules [7]. Furthermore, SPR is valuable in environmental monitoring, helping detect pollutants and pathogens in water and air [8]. Additionally, in food safety, it is used to identify contaminants and pathogens in food products, ensuring their safety for consumption [9]. Biosensors can be classified based on their configuration and mechanism, which determine how they interact with the analyte to produce a detectable signal. Optical biosensors are light-based interactions to detect the presence of analytes. Fluorescence-Based Biosensors rely on fluorescence emission from labeled molecules. Raman-Based Biosensors use Raman scattering for highly specific molecular identification and photonic Crystal-Based Biosensors detect shifts in light propagation within a photonic crystal [10].

Photonic crystals are periodic optical structures that influence the propagation of electromagnetic waves in a manner analogous to how periodic atomic lattices affect electron movement in solids. By forming a periodic variation of the refractive index, photonic crystals permit the fabrication of photonic bandgaps—frequency ranges over which specific wavelengths of light are prohibited from traveling [11]. This new attribute enables precise management of light transmission, making photonic crystals indispensable in modern optics and photonics [12].

Just as semiconductors control electron passage through energy band gaps, photonic crystals control photons by restricting or guiding their motion in specified frequency bands. This role facilitates a wide range of uses like optical waveguides, filters, sensors, and novel light-emitting devices [13]. By modifying their structural parameters, photonic crystals can be designed to produce excellent light confinement and dispersion management, which gives access to the creation of telecommunications, bio-sensing, and integrated photonic circuits [14].

Photonic crystals can be categorized by their dimensionality: one-dimensional (1D), two-dimensional (2D), and three-dimensional (3D) structures [15]. Each type exhibits unique properties that enable strong confinement of light within a very small volume, making them particularly effective at the nanoscale [15]. The ability to confine light so effectively has led to significant interest in PC sensors, which are recognized for their exceptional optical characteristics, including high sensitivity, compactness, rapid response times, resistance to electromagnetic interference, and cost-effectiveness [16].

The applications of photonic crystal sensors span various fields, including industrial and biomedical domains. They are capable of converting minute quantities of analytes into detectable signals, which is crucial for numerous sensing applications such as multiplexers, demultiplexers, lasers, optical fibers, logic gates, waveguides, and filters [17]. Moreover, these sensors function as transducers that convert detectable signals from one domain to another—exploring various domains such as electrical (current and voltage), biochemical (blood components and glucose), magnetic (magnetic fields), radiation (absorption and transmission), and mechanical (force and strain) [17].

In summary, the development of photonic crystals marks a significant advancement in optical technology. Their unique properties not only enhance the performance of optical devices but also open new avenues for research and application across multiple scientific fields. In our study, we reviewed several pieces of literature focused on bio-sensing applications and compared various structures with our proposed analysis. As a surface-sensitive technique, SPR requires only small sample volumes and delivers rapid results. This makes it particularly effective for bio-sensing, enabling faster diagnostic testing for pathogen identification, which is essential for medical diagnostics such as hemoglobin detection, dengue-malaria testing, blood glucose level and electro-chemicals.

1.2 Literature review

The integration of photonic devices has resulted in significant advances in sensing, communication and other optical applications [15]. An extensive review is presented on four principal components of modern photonic systems: fiber-based biosensors (including PCF-based and other variants), multilayer-based biosensors (prism-based and grating-based), and metal–insulator–metal (MIM) configurations [6]. The features, applications, and integration potential of each technology are examined, with particular emphasis on how their structural designs reveal persistent limitations and unresolved research gaps.

Optical fibers serve as the backbone of modern communication systems and have evolved significantly in the field of bio-sensing. Among the advanced designs, photonic crystal fibers (PCFs) have garnered attention due to their unique structural properties, such as controlled dispersion and high sensitivity to external refractive index changes [18]. These fibers feature microstructured air holes running along their length, enabling tailored light propagation characteristics as shown in figure 1.1a. On the contrary, fiber based sensors provide varying sensitivity levels, in practical applications often yield lower performance due to environmental factors. It also has a complex fabrication process which requires complicated tapering and coatings [19] .

The another category is multilayered based biosensor, this has two types one is 2D prism based biosensor and grating based biosensor shown in figure 1.1c and figure 1.1d. In prism based biosensor a plane polarized light strikes the prism at a certain angle that creates a total internal reflection and make optical excitation of the surface plasmons. Whereas, in grating based biosensor a light wave hits a metal grating from a dielectric medium to create surface plasmon waves which causes diffraction resulting in several waves that move away from the surface at different angle. These structures also have many disadvantages like complicated structure, lower sensitivity and weak surface functionalization.

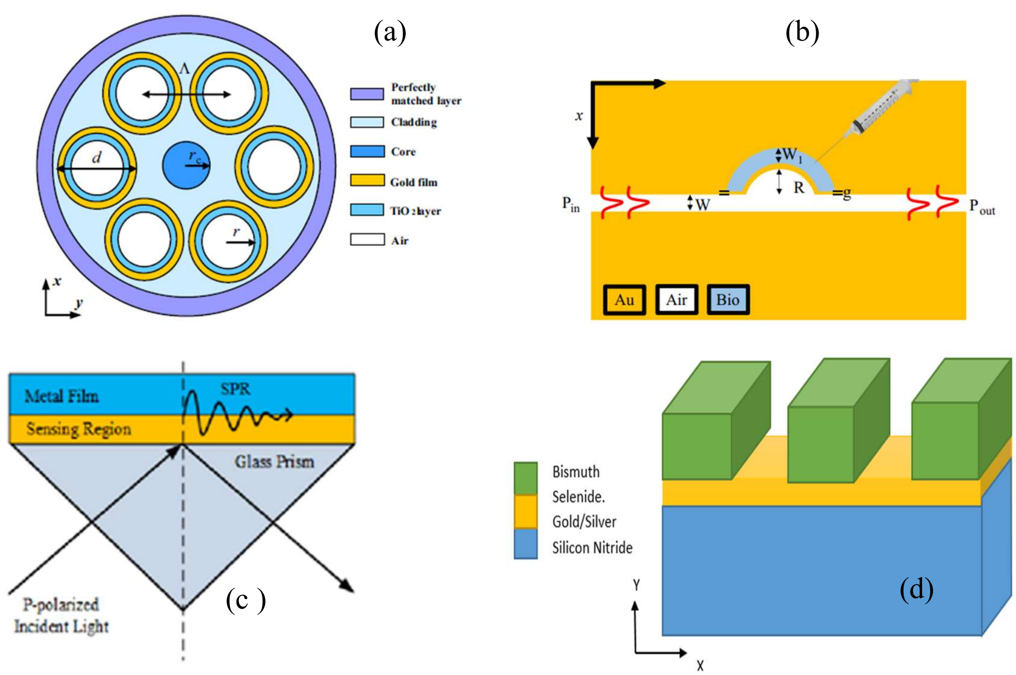

Figure 1.1: a. Multihole PCF biosensor [20] b. MIM waveguide based biosensor [21] c. Prism based [6] d. Metal dielectric grating structure [22].

Metal- Insulator- Metal MIM based sensors work at the boundary interface between metal and insulator which provides strong field confinement and improved light matter interactions as a result that enhances the surface plasmon polaritons as shown in figure 1.1b. Even though they offer great sensitivity and specificity it comes up with quite a few challenges, especially in materials, manufacturing scalability, coupling efficiency and design complexity [23].

The research by D. Gao [20] proposed a multi hole PCF biosensor detecting biomolecules has sensitivity of maximum 2000nm/RIU. It is coated with thin gold film and a TiO_2 film on the wall of the air holes. Although it has promising sensitivity it faces limitation related to the material thickness and the RI of the analytes being tested. Another research by A.K Goyal [24] used 1D-Photonic crystal cavity based structure designed by silicon (Si) material shows that the designed biosensor has lacking environmental stability, the materials thermal and mechanical stability is also not upright. The fabrication procedure is not discussed and its sensitivity is very poor of 323 nm/RIU and FWHM is 0.6nm. Additionally, the paper by S. Kumar [25] which is a prism based multilayered structure encompasses semiconductors and bimetallic gold and silver. The purpose is to detect glucose concentration in urine and has a sensitivity of 440 degree/RIU and FOM 90.65 only, at the wavelength range 1300-1800nm. The paper above has very less sensitivity, complicated structure, hard to fabricate, not biocompatible enough and expensive.

In 2023, S. Saurabh [26] designed a grating based sensor to detected glucose concentration in blood has a much lower sensitivity of 206.3nm/RIU and limit detection is 10^{-5} RIU in between the wavelength range 1.52-1.57 micrometer. It has propagation loss which affected the sensitivity, has complex structure that made field matter interaction challenging. The MIM structure based biosensor designed by Butt [21] detect biomolecules like blood, urine and bodily fluids at wavelength range from 800-1000nm. Although the sensitivity of it is

941.33nm/RIU it has challenges in light coupling issues, limited penetration depth, mode conversion complexity and the fabrication challenges.

We mainly researched on two unique structure biosensors, one is nanohole integrated MIM based SPR biosensor and the other one was MIM -grating based SPR biosensor.

Compared to all other biosensors mentioned above our first proposed work has the easiest structure containing nanomaterials Silver and Titanium only. It is the most available photoactivated nanomaterials found and the very cheapest among all the above materials mentioned in other papers. It has a nice analyte chamber which is a nanocavity based hole structure, it causes the analyte to interact with the photonic nanomaterials efficiently. It boosts the electric field's strength as light goes through the titanium and silver thin film and the sample. Because of this, we achieve a highest sensitivity of 515.2 nm/RIU allowing us to detect Hb in blood and other biomolecules at the wavelength range 450-700nm.

Moreover, our investigated nanohole array integrated MIM based structure has a structure that employs dual mode surface plasmon resonance sensor. This design offers several advancements over earlier photonic crystal and plasmonic biosensors. It has superior Sensitivity, simplified fabrication and structural optimization, is biocompatible and has cost effective materials. All of those above structures go through very complicated production processes, including sample preparation whereas our proposed structure is simple and easy to handle. Below table 1.1 shows the comparative analysis of the different types of biosensors and their sensitivity.

Table 1.1: Comparison analysis of different types of biosensor and their sensitivity.

References	Year	Biosensor structure type	Materials	Analyte	Sensitivity (nm/RIU)	FOM/ FWHM(nm)
[20]	2014	Multihole PCF based structure	Thin gold film +TiO2 coated air hole walls	Biomolecules	2000nm/RIU	-/-
[24]	2020	1D photonic crystal cavity (Si based) structure	Silicon-based photonic crystal structure	General bio-sensing	323nm/RIU	-/0.6nm
[25]	2024	Prism based multilayered structure	Au-Ag bimetallic +semiconductors	Urine glucose	440deg/RIU	90.65/-
[26]	2023	Grating based structure	SiO2 based	Blood glucose	206.3nm/RIU	-/-
[21]	2023	Metal insulator metal MIM based with semicircular coupled with semi cavity	Air and gold	Blood,urine, bodily fluid.	941.33nm/RIU	-/-

SPR is highly sensitive to changes in the refractive index of the medium near the metal surface. Therefore, in recent years, it has received keen attention in bio-sensing applications since various biomaterials, liquid analytes, gasses, nucleic acids and proteins have specific RI. This feature facilitates convenient sensing of their RI change, allowing for easy detection with high sensitivity [27]. As a result, biosensors play a crucial role in medical diagnostics, point of care testing, environmental testing, food safety, bioprocess monitoring, drug discovery and forensic analysis [28]. For instance, they have been used for detecting several diseases, blood component detection, glucose detection in urine and blood, protein detection, cancerous cell, virus and bacteria.

Recent paper [29] which is a MIM based SPR biosensor has elliptical resonators on silver material. It detects hemoglobin concentration in blood of sensitivity of 1100 nm/RIU. Although it has high sensitivity, its complex structure causes challenges in fabrication and its resonator's performance can be affected by temperature, noise or external interference. Additionally, the paper [25] MIM based multilayered bimetallic, semiconductor and 2D nanomaterials is used to detect glucose concentration in urine. And also the paper [30] metal-nitride layers on a bimetallic (Au-Ag) SPR biosensor is used to detect urine glucose. Although both have sensitivity of 440 degree/RIU and 411 degree/RIU compared to our proposed work, it has very less sensitivity, complicated structure, hard to fabricate, not biocompatible enough and costly. Another recent paper [31] which is multilayered grating based SPR biosensors of plasmonics Cytop Polymer grating structure with periodicity comparable to the incident wavelength are applied to evaluate the plasmonics Talbot biosensor. It operates with a sensitivity of 324 nm/RIU which is very less compared to our proposed sensor. Moreover, our proposed structure is biocompatible, easy to fabricate and cost effective. The mentioned paper has not examined any particular biomolecules numerically whereas our biosensor can detect Hb hemoglobin in blood and the results are mentioned.

In recent years, plasmonic biosensors have been the most researched sector, as many SPR based integrated biosensor devices have been launched to support the medical sector [32]. This study introduces a simple cavity coupled plasmonic biosensor, which can be rapidly fabricated to get a label free, real time, sterile, reusable device with high sensitivity. This miniature structure with microcavities of the plasmonic nanostructure significantly impact its performance by boosting the sensitivity and resolution while requiring minimum sample volume.

Additionally, two separate grating based MIM structure biosensor were designed using an insulator, bismuth selenide. Bismuth Selenide is a material with exceptional sensitivity and optoelectronic properties, making it highly suitable for bio-sensing applications [33]. As highlighted in the work of S. Wang [34], the plasmonic and surface properties of Bi_2Se_3 outperform traditional insulators.

In 2023 a paper by S. Saurabh [23] investigated a grating based sensor which has detected glucose concentration in blood which has a much lower sensitivity of 206.3nm/RIU than our proposed structure. Suthanthiraraj [35] created an on-chip LSPR biosensor that can detect dengue NS1 antigen with a sensitivity of 9 nm/(μg/mL). Huang [36] also reported an LSPR on chip gold nanoparticle biosensor that uses a microfluidic device to detect biotin/antibody, showing a sensitivity of about 100 nm/RIU. Another paper by S. Raga [37] where the biosensor is featured of Gallium arsenide (GaAs) composite semi-conductive rods which has a complex structure to detect malaria. On the contrary, our biosensor is easy to design and it is used for multiple detections, which shows that it can detect a wide range of RI of analytes. Not only that it has achieved high sensitivity of 1035.8nm/RIU. All of those above structures go through very complicated production processes, including sample preparation whereas our proposed structure is simple and easy to handle.

1.3 Motivation of the study

Biosensors are important tools in areas like medicine, environmental science, food monitoring, and biotech. They help with early disease finding, quick testing, making sure our environment is safe, and keeping food high in standards. Biosensors can be used in so many ways, we studied and simulated to find hemoglobin levels in blood, mosquito-related sicknesses like dengue and malaria, and glucose, sodium, and potassium levels. There aren't any vaccines for these diseases, finding them early is very important for saving lives. Also, glucose, sodium, and potassium are very important for keeping our health and body balanced. If we can detect these markers with one biosensor, health monitoring would improve and diseases could be found earlier. Current methods for detecting biomolecules such as Hb, glucose, and electrolytes often depend on costly and time intensive procedures like PCR. Our goal is to create a label free, reagent-free, non-invasive biosensor. Many standard biosensors have drawbacks such as low sensitivity, complicated manufacturing and an inability to detect various biomolecules at the same time. These limitations make quick point of care diagnostics hard, especially in distant locations. These issues led us to investigate creating a very sensitive, miniaturized and affordable SPR biosensor using MIM based biosensor that uses grating and nanohole structures.

1.4 Objectives with specific aims and possible outcomes

The objectives of this thesis are as follows:

1. To design and simulate nano-hole array integrated MIM based SPR sensor for detecting hemoglobin in blood.
2. To design and simulate MIM - Grating Based SPR biosensor using metal-bismuth selenide (Bi_2Se_3)- silicon nitride (Si_3N_4) for Dengue, Malaria, Glucose, and Electrolyte Detection
3. Perform dimension optimization to identify optimal structure.
4. Determine performance matrices such as sensitivity, quality factor, detection accuracy and FWHM.
5. Design highly sensitive, reliable and portable biosensor.
6. Investigate practical /fabrication feasibility, and scalability.

Specific outcomes

1. Design an advanced plasmonic biosensor capable of efficient operation in the visible range and infrared (IR) spectral range which particularly well-suited for biological sensing applications.
2. Detect biological parameters such as blood hemoglobin concentration, mosquito-borne diseases (e.g., malaria and dengue) in the human body and glucose and electrolytes concentration.
3. Ensure ease of fabrication and effective detection of biological analytes, while maintaining cost efficiency and adaptability for practical, real-world deployment.

1.5 Methodology

Initially, we designed grating-based structures, including different dimensions' grating's to get the optimum structure. Using specific structural parameters, we developed both metal-dielectric-metal and dielectric-metal-dielectric configurations incorporating various photonic crystals and metallic materials. Next, we selected the source frequency and polarization angle that yielded the highest output. For refractive index values ranging from 1.3 to 1.5, we adjusted the source frequency to determine the optimal resonance wavelength. By analyzing transmission and reflection results, we identified the structure and material combination that provided the best resonance performance, ultimately achieving our desired outcome. The source polarization and central frequency play a crucial role in identifying the optimal frequency for the selected biosensor. Once determined, it becomes easier to analyze the resonant patterns and optimize the overall structure size. We finalized a structure and continued refining it to achieve optimal transmission and reflectance over a broader bandwidth until the desired outcomes were met. At this stage, we optimized the area and conducted further simulations using the most suitable materials. Finally, simulations were performed with various metals and compounds such as tungsten, nickel, titanium, and bismuth selenide, as well as photonic crystals like gold and silver, to compare their transmission and reflectance properties. The flowchart shown in figure 1.2 shows the main steps we followed to design our biosensor.

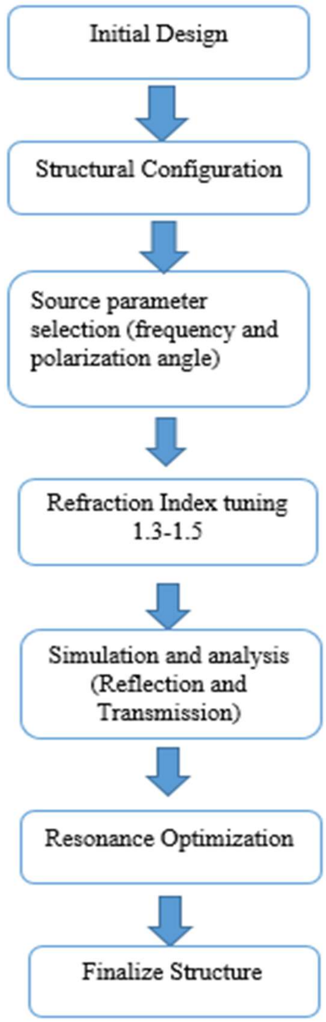

Figure 1.2: Steps to design photonic biosensor.

1.6 Thesis structure overview

Chapter 1 introduces the concept of photonic crystal SPR-based biosensors. It evaluates previous results to identify areas for improvement and define our research objectives and methodology. The chapter concludes with a summary of the thesis.

Chapter 2 covers the basic theories of surface plasmon resonance SPR and its mathematical background. It shows the derivation of SPP dispersion relation by using Maxwell's equation on metal-dielectric boundary. Then it explains how excitation occurs on different structures and some other mathematical parameters are discussed.

Chapter 3 focuses on the design methodology of the nanohole or cavity-based MIM structure biosensor. This chapter presents the simulation conditions, fabrication process, and a comparative analysis with similar prior works. Later, hemoglobin concentration of blood is examined.

Similarly, Chapter 4 explores the grating-based MIM structure biosensor, where two different designs were tested while keeping the materials consistent. This chapter discusses the simulation setup, results, and fabrication process of the biosensor. Subsequently, dengue malaria as well as glucose and electrolytes concentration in blood were diagnosed.

Finally, Chapter 5 summarizes the research's result, confirming that the research objectives were achieved. It also highlights challenges encountered in the development of grating and SPR-based biosensors and suggests potential directions for future research.

Chapter 2

Theory Analysis

2.1 Introduction

This chapter presents the basic theories of surface plasmon resonance SPR and its mathematical underpinnings. It details the SPP dispersion relation's derivation using Maxwell's equations at a metal- dielectric interface. Following this, it goes over excitation methods for different structures and discusses related mathematical parameters.

2.2 SPR excitation and dispersion correlation

Surface plasmon resonance (SPR) is a phenomenon that occurs when the momentum of incident photons matches the momentum of surface plasmons, leading to a resonance condition. This resonance results in a sharp dip in the intensity of reflected light and is highly sensitive to changes in the refractive index of the medium near the metal surface. SPR is commonly observed when light is incident on a thin metal film, typically at a specific angle, and excites collective oscillations of free electrons at the metal-dielectric interface, known as surface plasmons [38].

2.2.1 Surface plasmon at metal and dielectric interface.

First we must know what plasmon and polariton. Plasmon is a type of quasiparticle that comes from the oscillation of plasma. It's like how photons are the packets of light. On the other hand, a polariton is actually a wave created by the positive and negative charges moving together. When plasmon interacts with photons, they form some plasmon polaritons. Specifically, Surface plasmons are those that are stuck to surfaces and have a strong interaction with light, leading to the creation of a polariton [38].

2.2.2 Maxwell's equation

SPR happens when surface electromagnetic waves known as surface plasmons move along the edge of a metal and dielectric. These waves come from solutions to Maxwell's equations when certain conditions are met. The free electron oscillation in metals can be analyzed using these equations [25].

$$\nabla \cdot \mathbf{D} = \rho_{ext} \qquad (2.1)$$

$$\nabla \cdot \boldsymbol{B} = 0 \qquad (2.2)$$

$$\nabla \times \boldsymbol{E} = \frac{-\partial \mathrm{B}}{\partial t} \qquad (2.3)$$

$$\nabla \times \boldsymbol{H} = J_{ext} + \frac{\partial D}{\partial t} \qquad (2.4)$$

Here, D= dielectric displacement, B= magnetic field, E= electric field and ρ_{ext}= the external charge, J_{ext}= current densities, P= electric dipole moment. They can be written in the form below.

$$\boldsymbol{D} = \varepsilon_0 \boldsymbol{E} + \boldsymbol{P} \qquad (2.5)$$

$$\boldsymbol{H} = \frac{1}{\mu_0}\boldsymbol{B} - \boldsymbol{M} \qquad (2.6)$$

2.2.3 The Drude Model: free electron behavior in metals

The Drude model is a classical approach to describing the optical and electrical properties of metals. It treats conduction electrons as a gas of non-interacting particles that undergo collisions with a fixed background of positively charged ions. According to the Drude model, the dielectric function of an ideal free electron metal is given by the equation [38].

$$\mathcal{E}_m(\omega) = 1 - \frac{\omega_p^2}{\omega^2 + i\gamma\omega} \qquad (2.7)$$

$$\omega_p = \sqrt{\frac{\mathrm{N}e^2}{\mathcal{E}_0 m_e}} \qquad (2.8)$$

Here , ω_p is the plasma frequency, N is the free electron density, e is the elementary charge of the electron, ε_0 is the permittivity of free space (For metals, $\varepsilon_\infty \approx 1$,) and m_e is the electron's effective mass. The damping term γ gamma accounts for electron scattering within the metal [38]. The Drude model is fundamental to understanding SPR because it determines how metals interact with electromagnetic waves, leading to the excitation of surface plasmons. All the equations from 2.1 to 2.8 are explained elaborately by Xiaoou Mao in his paper [38].

2.3 Excitation of SPP

Surface plasmon resonance excitation involves coupling light energy to surface plasmons which are collective oscillations of electrons at the interface between a metal and a dielectric material. Since the momentum of photons in free space is typically less than that of surface plasmons, direct excitation by light is not possible necessitating special techniques to achieve phase matching [38].One common method is prism coupling. It uses a prism to increase the momentum of incident light. In the kretschmann configuration a thin metal film is deposited on a prism and light is directed through the prism onto the metal film. At a certain angle, the light's momentum matches the surface plasmons which causes the SPR effect. You can see this as a sharp drop in the intensity of the reflected light. There is also an otto setup which is a bit similar but has a smaller air gap between the prism and metal [38].

SPP cannot be directly excited by light beams on a flat metal dielectric interface because the propagation constant is greater than the wave vector $\beta > k$. As a result, the component of the momentum along the interface of photons striking the surface at an angle θ to the normal is less than the SPPs propagation constant β, even at very shallow angles, preventing phase matching.

However, due to inherent momentum mismatch between light in free space and surface plasmons, external coupling techniques such as prism coupling (Kretschmann and Otto configurations) or grating coupling are necessary to provide additional momentum [39]. Therefore, phase-matching to SPPs can be achieved in a three-layer system consisting of a thin metal film sandwiched between two insulators of different dielectric constants as shown in figure 2.1a and 2.1b. Light is reflected at a metal surface covered with a dielectric medium (ε_0>1) usually in the form of a prism. This high-refractive-index prism enables total internal reflection, generating an evanescent wave that penetrates the metal layer and excites SPR.

$$k_x = \frac{\omega}{c} \left(\sqrt{\varepsilon_0} \right) sin\theta \qquad (2.9)$$

Where, ε_0 prism is the dielectric constant of the prism. When resonance occurs, a sharp dip in reflected light intensity is observed, which can be used for bio sensing applications.

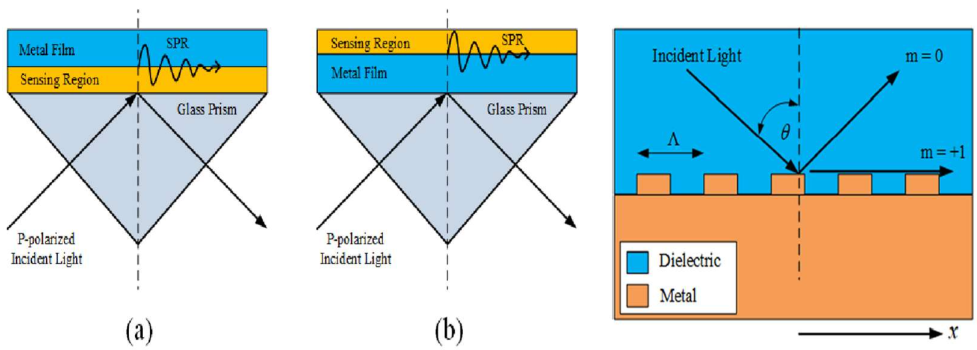

(a) (b) (c)

Figure 2.1: a. Otto configuration [6] b. Kretschmann configuration [6] c. Metal Dielectric grating structure [6].

Another way to do this is grating coupling. This method involves creating a grating structure as shown in figure 2.1c on the metal surface that adds extra momentum we need for phase matching. The grating helps the incoming light pair up with the surface plasmons by introducing a specific vector. Here, SPPs are excited by adding a reciprocal lattice vector from grating.

The matching condition is based on a simple equation [6] involving the angle of incident light, where k_x is the propagation constant of the non-diffractive optical light wave, m is the diffraction order $m = 0, \pm1, \pm2, \pm3, \ldots$, Λ is the grating period and n_d is the refractive index of the dielectric

$$k_d = k_x + mG = \frac{2\pi}{\lambda} n_d \sin\theta + m \frac{2\pi}{\Lambda} \qquad (2.10)$$

Our first investigation shows that, when light passes over the photonic crystal from one end it interacted with the blood and get detected from another end. The propagation of light varied in the photonic crystal depending on the refractive indices of the blood analyte [40]. When the incident light energy couples with the metal-dielectric layers, electrons of it result in changes in the reflectance or transmittance of the incident light. Free electrons at the silver nanohole boundaries must oscillate coherently for SPR to function. For this oscillation, the relationship between the wave vector (k_{SP}) and frequency (ω) can be represented in equation 2.11 as follows.

$$k_{SP} = \frac{\omega}{c}\sqrt{\frac{\varepsilon_m(\omega) n_a^2}{\varepsilon_m(\omega) + n_a^2}} \qquad (2.11)$$

Where, n_a is the refractive index of the medium inside the cavity, c is the speed of light and $\varepsilon_m(\omega)$ is the silver nanohole's dielectric function. We can represent the complex dielectric function below using the Drude model using equation 2.12.

$$\varepsilon_m(\omega) = 1 - \frac{{\Omega_P}^2}{\omega^2 + i\omega\gamma_0} \qquad (2.12)$$

Here, γ_0 is the damping constant of the silver layer and Ω_P represents the plasma frequency. We use the values $\Omega_P = 1.375 \times 10^{16}$ rad/s and $\gamma_0 = 3.12 \times 10^{13}$ rad/s from reference [41].

Stable oscillation now requires the wave vectors of the plasmon polaritons and the incident light to match. The wave in the grating surface can be represented by the wave vector shown by equation 2.13 as follows:

$$k_d = \frac{\omega}{c} n_a sin\theta + m\frac{2\pi}{P} \qquad (2.13)$$

Where, θ is the light incidence angle, *m* is the diffraction order (0, ±1, ±2…), *c* is the speed of light and P is the period of the grating.

So, the resonance condition is written by equation 2.14 as follows:

$$Re\{k_{SP}\} = \frac{\omega}{c} n_a sin\theta + m\frac{2\pi}{P} \qquad (2.14)$$

For metals like silver the real part of the metallic dielectric function is much greater than the imaginary part. So we can use the following by equation 2.15:

$$Re(k_{SP}) \simeq \frac{\omega}{c}\sqrt{\frac{\varepsilon_m(\omega) n_a^2}{\varepsilon_m(\omega)+n_a^2}} \qquad (2.15)$$

Linking the above equations we get the resonance equation:

$$n_a^2\omega^4P^2 + \{(\gamma_0{}^2 - \Omega_P{}^2)P^2 n_a{}^2 - 4\pi^2m^2c^2(1+n_a^2)\}\omega^2 - 4\pi^2m^2c^2(\gamma_0{}^2 - \Omega_P{}^2 + \gamma_0{}^2 n_a{}^2) = 0 \qquad (2.16)$$

Equation 2.16 greatly depends on the refractive index inside the cavity (n_a) as expected. If the refractive index is changed inside the cavity, the resonance wavelength changes. Using the values of $\Omega_P = 1.375 \times 10^{16}$ rad/s, $\gamma_0 = 3.12 \times 10^{13}$ rad/s, $n_a = 1.3$ we get, $\omega^2 = 7.2511 \times 10^{30}$ rad^2/s^2 using resonance wavelength $\left(\lambda = \frac{2\pi c}{\omega}\right)$ we get 700.2nm. The resonance wavelength for refractive index 1.3 is 585 nm which is closest to our theoretical analysis. Therefore, the resonance wavelength increases if the refractive index is increased.

2.4 Mathematical parameters

Different methods have been created to build surface plasmon biosensors that work well and are easier to produce. Key performance parameters such as figure of merit (FOM), detection accuracy (DA), operating refractive index RI, wavelength range, full width at half maximum (FWHM) and the sensor performances Quality Factor (Q-factor), Wavelength Sensitivity(S), Resolution, and Transmission efficiency are evaluated to optimize the quality and overall performance of these sensors [23].

In our study we only focused on resonance wavelength, sensitivity, detection accuracy, FWHM and quality factor. The sensitivity (S) is the ratio of obtained change in the resonant wavelength due to change in the refractive index. Here, where $\Delta\lambda$ is change in resonant wavelength and Δn is change in refractive index. Sensitivity is to be measured in terms of nm/RIU and it should be as high as possible.

$$S=\frac{\Delta\lambda}{\Delta n} \qquad (2.17)$$

The Quality factor (Q) is defined as the ratio of obtained resonant wavelength to change in the wavelength at Full Width Half Maximum (FWHM). Q should be as high as possible and it is a unit-less parameter. The sensor's quality factor depends on both Sensitivity and FWHM, it can be expressed by,

$$Q = \frac{S}{FWHM} \qquad (2.18)$$

The sensor's Detection accuracy is the reciprocal value of full width half maxima. It is a unit-less parameter. FWHM is the width of the resonance peak at the half of the maximum value. It is calculated by,

$$DA = \frac{1}{FWHM} \qquad (2.19)$$

Scientists are diligently striving on bettering these metrics by suggesting different device designs that balance sensor sensitivity and ease of production. They are looking at new materials like 2D and organic ones, as well as various shapes such optical fiber-based, discrete multilayer, compact metal-insulator-metal, or grating-based designs. They are also focusing on how to excite surface plasmons effectively and where to place input and output ports to make these biosensors work better.

2.5 Conclusion

We methodically looked at the basic ideas and mathematical foundations of the suggested biosensor design in this theoretical analysis. The theoretical base gives solid backing for upcoming simulation which makes sure the design is both scientifically correct and practically feasible.

Chapter 3

Nanohole array integrated metal insulator metal MIM based dual mode SPR sensor for detecting hemoglobin in blood

3.1 Introduction

Chapter 3, details the material choice, simulation for device configuration, study of transmission spectra and performance and then biosensor's use for detecting hemoglobin in blood. This chapter looks into a new way to design a surface plasmon resonance (SPR)-based optical biosensor capable of detecting minor changes in the refractive index. This research focuses on a nanohole array integrated- MIM based biosensor that incorporates silver and titanium to achieve SPR resonance. At first materials were selected by conducting extensive simulations on three different configurations using three different materials to identify the optimized structure and material combination with the highest sensitivity. A key innovation of our design is its nano-hole-shaped grating on metal-insulator-metal (MIM)based structure and its dual mode SPR sensitivity. To evaluate material performance, we investigated the effects of nickel, tungsten, and titanium under various light wavelengths. Our findings revealed that titanium outperforms nickel and tungsten, offering superior resistance to oxidation, excellent biocompatibility, and enhanced durability qualities that make it well-suited for biosensor fabrication and clinical applications. Additionally, we optimized the biosensor's structure by modifying the nanohole dimensions and the array pattern etched into the silver layer, leading to an innovative plasmonic structure. This design promotes coupling effects between metallic nanoparticles, resulting in a wavelength shift in plasmon resonance modes, facilitating optical transmission and improved detection performance. As a result, it has achieved the highest sensitivity of 515.2 nm/RIU. Moreover, it provides dual mode SPR sensitivity which leads to more accurate detection and allows simultaneous monitoring of various biomarkers. After finalizing the optimized structure, oxygenated hemoglobin concentration in blood is detected. The research investigates a range of hemoglobin (Hb) concentrations from 0 to 60 g/dl, simulating diverse blood conditions. The refractive index at the resonant wavelength varies between 1.335 and 1.344, depending on the specific Hb concentration. Additionally, our biosensor is compared with other papers and concluded that the proposed grating-based Surface Plasmon Resonance (SPR) biosensor offers a novel approach for detecting hemoglobin (Hb) with high sensitivity and specificity. Finally, we discussed the fabrication process of our proposed structure. Numerical simulations were performed in ANSYS Lumerical FDTD solution 8.19.1584 version [42]. Performance parameters such as transmission, reflection, full-width at half-maximum (FWHM) and quality factor were analyzed to assess detection accuracy.

3.2 Structural design and sensing mechanism

In this study, we have designed a cavity coupled waveguide biosensor using Silver (Ag) and Titanium (Ti) which will act as a well effective tool to detect Hb concentration in modern health care services. Several quantifiable techniques have been developed to determine the integral, local, or average RI of single living cells or multiple cells using digital holographic microscopy [27], optical trapping technique [43], integrated chip technique [44], Hilbert phase microscopy [45], tomographic phase microscopy [46], tomographic bright field microscopy [47]and several interferometry techniques [48].

Blood, a vital bodily fluid, plays a critical role in oxygen and nutrient transport, as well as waste removal [40]. Blood optics, essential for biophotonic and clinical applications in therapy and diagnostics [49], includes diagnostic methods based on Mie theory, leveraging light scattering and absorption properties of human blood [50]. The light absorption and scattering characteristics of blood depend on erythrocyte refractive index, largely influenced by hemoglobin concentration [49]. Variations in Hemoglobin concentration can lead to conditions such as anemia, polycythemia, and other hematological disorders, underscoring the need for accurate detection methods.

Early detection of abnormal Hb levels can significantly impact patient outcomes, potentially preventing postoperative hemorrhages and enabling timely interventions [51]. Our biosensor aims to contribute to these efforts by offering sensitive and specific measurements of Hb hemoglobin concentration, thereby potentially saving lives through early intervention. Figure 3.1 shows the XY plane simulation view and schematic representation of the biosensor.

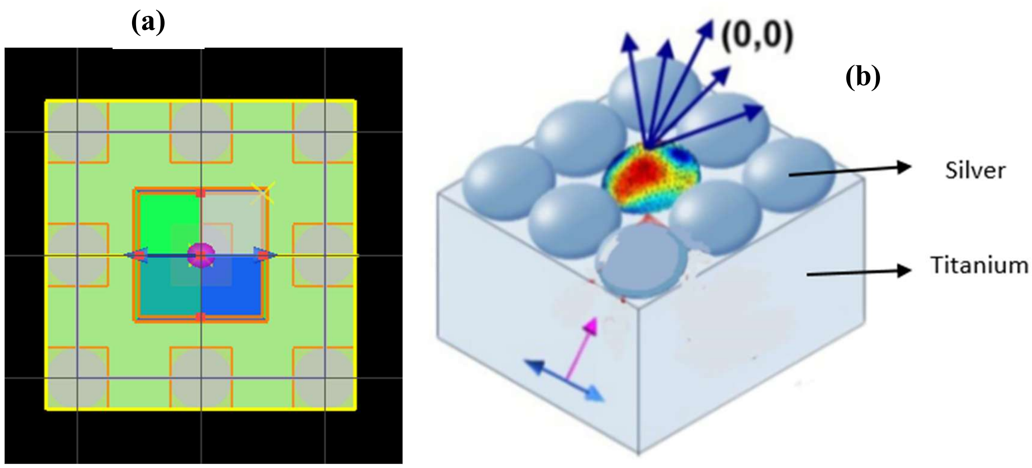

Figure 3.1: (a)XY plane of simulation view, (b) Schematic representation of the biosensor when the light source is projected, SPR base transmission shifting is taking place and the monitor from above is capturing the spectrum (Inset blue arrow shows the direction of TFSF source and pink arrow indicates the direction of plane wave).

3.3 Material selection

Although there are other different metals which have high sensitivity, they are very expensive in terms of mass production of Hb detection sensors. Also, some of these metals are not biocompatible enough, have lack of antimicrobial properties and are susceptible to corrosion, which can affect the environment and the stability and durability of the sensor.

Here, we investigate the optical properties of metal dielectric plasmonic substrates for refractive index sensing. Here we used Silver (Ag) and Titanium (Ti) metals where nanohole arrays are etched in a silver metal layer. Silver is a native metal which is cheap, highly reflective across a broad range of wavelengths particularly in the visible and near-infrared regions and has excellent conductivity properties. It exhibits antibacterial properties too.

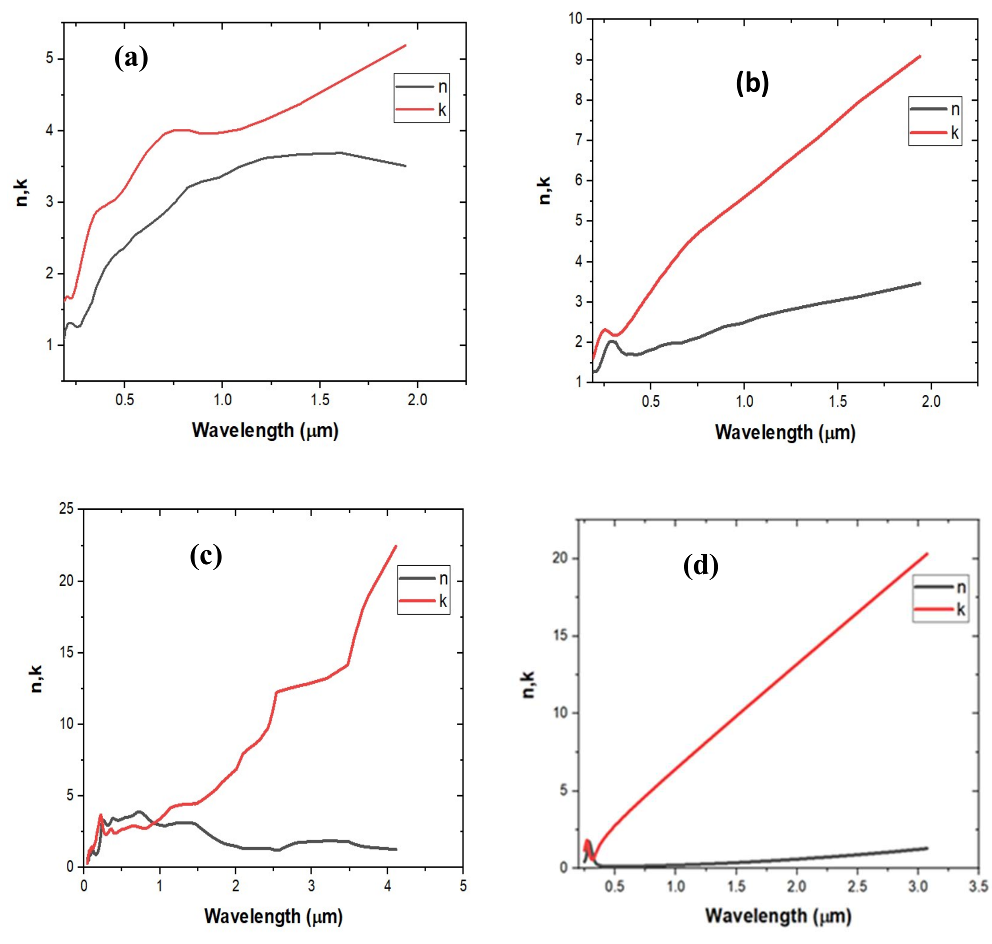

Figure 3.2: Real and imaginary part of refractive index a. Nickel b. Titanium c. Tungsten d. Silver.

Moreover, Titanium (Ti) is biocompatible, corrosion resistant and mechanically very strong. Combining these materials results in the design of a biosensor which enhances the performance, biocompatibility and durability of the sensor.

On the contrary, silver has oxidation properties which is a limitation for this biosensor. Here, the high sensitivity of resonant coupling mode between SPR from Silver Titanium (Ag Ti)-nanohole arrays and LSP [52] from Silver (Ag) nanoparticles to changes in the environment's refractive index variations is observed during the investigation.

Other than Titanium we worked on Nickel (Ni) and Tungsten (W) also to check their sensitivity in-between refractive index 1.30 and 1.40 as shown in table 3.1. We preferred Titanium over Nickel (Ni) and Tungsten (W) not only because of their sensitivity but due to its good material properties. Nickel has limited transparency, low reflectivity and is susceptible to corrosion due to oxidizing effect. Moreover, Tungsten has high density, brittleness and has more oxidizing effect than all. Therefore, Titanium exhibits highest resistance to oxidizing among these three and has good biocompatibility, strength, durability for fabrication to biosensor devices which can be handled and operated in a clinical setting easily. The real and imaginary part of the refractive index of nickel, titanium and tungsten are shown in figure 3.2 (a-c).

Moreover, ensuring the long-term stability and durability of SPR biosensors is a significant challenge. Degradation of materials or photonic structures over time can lead to reduced performance. Therefore, regular maintenance and recalibration may be necessary to maintain sensor accuracy, which can be time-consuming and costly. Additionally, the interaction between biological molecules like Hb hemoglobin and the sensor surface can lead to biofouling. To improve biocompatibility and minimize degradation of materials over time possible solutions could be to go for a coating method. There are several coating methods like Polyethylene glycol (PEG) coating, biomolecule coating, protein coating and carbon based coating [2]. Despite its benefits, these coatings can extant challenges. The stability of the coating layer's conditions can be variable, potentially leading to degradation over time.

Additionally, achieving uniform and stable coatings can lead to complexity and increase the cost of sensor fabrication. Figure 3.3 (a-c) shows the sensitivity analysis of all materials.

Table 3.1: Comparison of sensitivity when changing the bottom layer material while keeping the top layer material constant.

Top layer	Bottom layer	Sensitivity (nm/RIU)
Silver	Tungsten	343.44nm
Silver	Titanium	404.34nm
Silver	Nickel	386.36nm

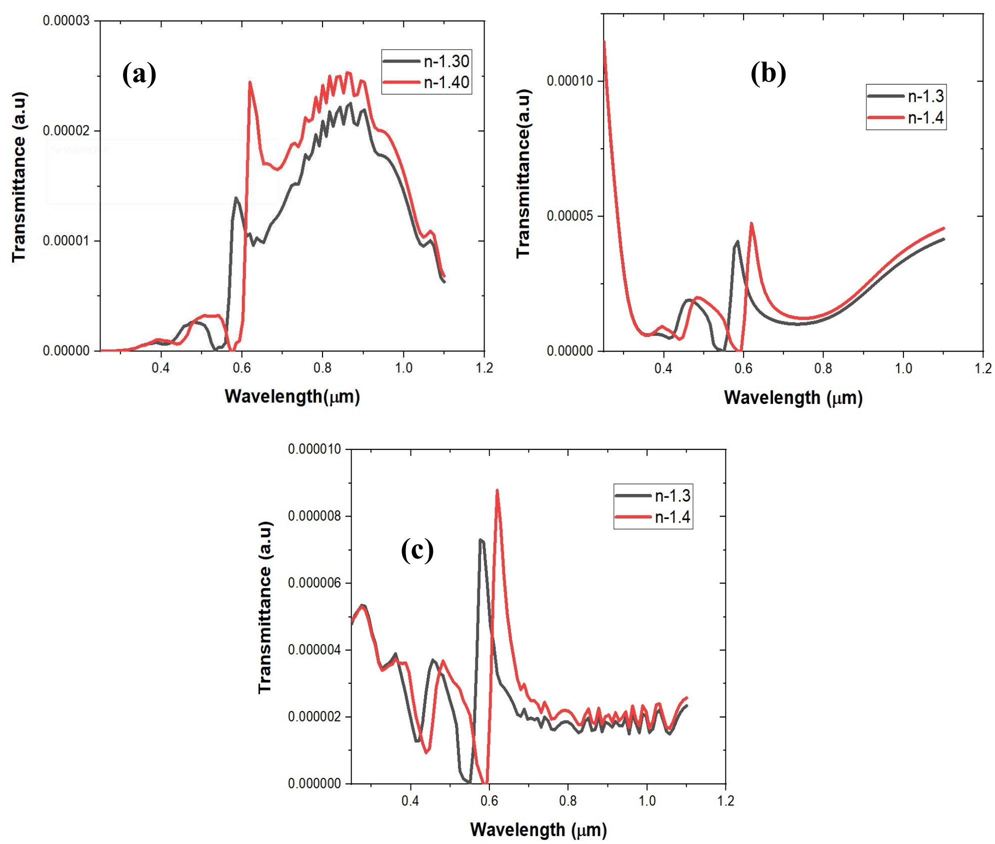

Figure 3.3: Transmittance (sensitivity) analysis of (a) Tungsten, (b) Titanium, and (c) Nickel.

3.4 Device structure and simulation parameters

Our design embraces a simple manufacturing procedure with non-complicated sample-controlling techniques. A fundamental issue in plasmonic resonance sensors is coupling the surface plasmon with an optical wave in free space, because the plasmonic wave vector is substantially bigger than the free-space wave vector, which causes the momentum mismatch between light and surface plasmon [53]. In this study we employed ANSYS Lumerical FDTD solution 8.19.1584 version. Here, figure 3.4 (a) and (b) demonstrate the design of the 1D grating structure which consists of nanoholes arrays of diameter 200 nm etched over silver (Ag) layer which is 100 nm thick. The silver layer is placed on 950 nm of titanium (Ti) substrate film. After a series of research and experiments these layers with specified dimensions have been determined to design a novel plasmonic structure figure 3.4c.

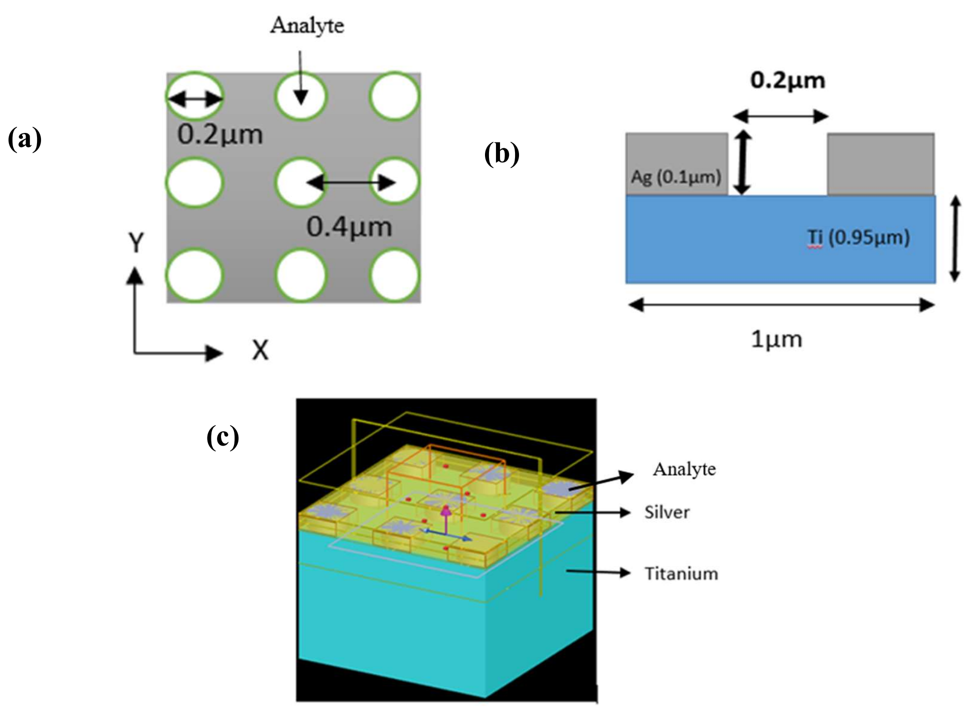

Figure 3.4: (a) 1D illustration for the simulation model in x-y plane (b) unit cell design in x-z plane and (c) Perspective view for simulation (Inset blue arrow shows the direction of TFSF source and pink arrow indicates the direction of plane wave).

The plasmon coupling effect is demonstrated by the introduction of nanohole arrays in the silver layer. A stronger plasmonic near field coupling between two metallic nanoparticles results in a distance-dependent wavelength shift of the plasmon mode [54]. These resonance modes cause optical transmission at wavelengths between 450nm -700nm.

Here, to simulate optical reflection and transmission data of the structure, an optical power monitor is placed in between the source and upper PML boundary [42]. Here we studied transmission from plasmonic structure for a normal Electromagnetic incidence light in the wavelength range from 450 to 700 nm. For the experiment, at first the refractive index was selected from 1.20 to 1.45 and then the above parameters were observed so that the sensing refractive index for hemoglobin concentration can give desired results.

In paper [55] we can see a two layer grating based sensor using silicon and silicon dioxide. Here, for three-waveguide thickness of silicon layer (220 nm, 150 nm, and 100 nm) the bio-sensing capability is evaluated. It is found that the sensor with a 100 nm thickness provides a higher sensitivity of 322.96 nm/RIU than all other designed structures mentioned in the paper. It has been also assessed that the higher gap width period 440 nm between the gratings has more sensitivity. Compared to the above paper our novel structure has a thickness of 100 nm of silver photonic layer and the gap between the periods is 400 nm which results in the highest sensitivity of 515.2 nm/RIU. This shows that our structure can exhibit better results flexibly than other parametric structures.

Table 3.2 shows the dimension and structure details.

Table 3.2: Structure and dimension details

Layers dimension	Material	Purpose
Top layer: length=1000 nm, width=1000 nm, thickness=100 nm Nanohole's in a silver layer, diameter= 200 nm, period =400 nm	Silver	Lights interact with the nanoholes which are etched in silver and create resonance.
Bottom layer: length= 1000 nm, width=1000 nm, thickness=950 nm	Titanium	Works as a substrate.

Although we have examined the sensitivity by altering the thickness, period and diameter of nanoholes on our structure we obtained optimum parameters of the structure which provides good fabrication feasibility and sensitivity. Compared to the mentioned paper our investigation has 37.28% more improved sensitivity.

3.5 Result analysis and numerical discussion

As discussed, the simulation results of the nano hole cavity under z-polarized illumination across a wavelength range spanning from 450 nm to 700 nm is observed. The transmission spectra of the silver titanium nanohole array are shown in figure 3.5, with the analyte's refractive index varying from 1.25 to 1.45.

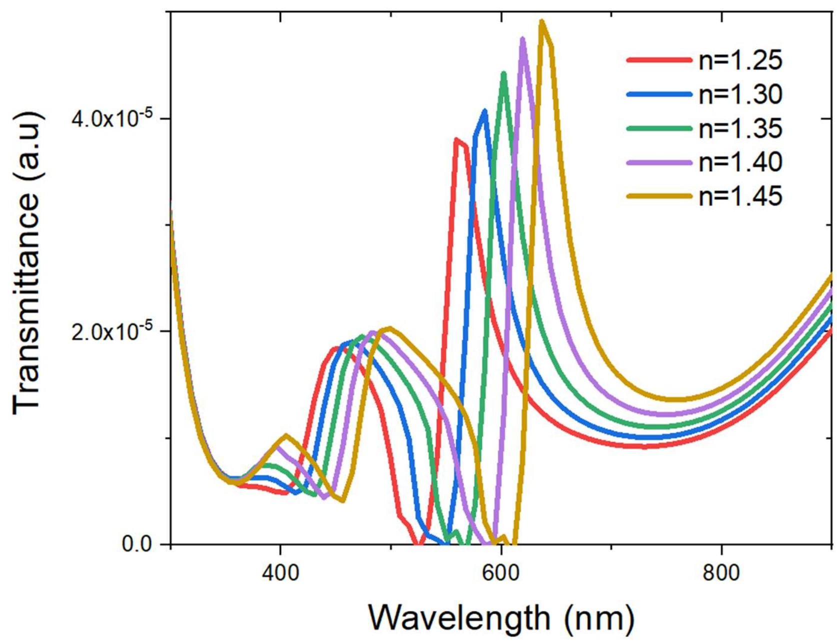

Figure 3.5: Transmittance vs wavelength graph.

The Sensitivity, FWHM, Detection accuracy and Quality factor has been calculated and shown in table 3.3.

Table 3.3: (a) sensitivity at mode 1 and mode 2 (b)parameters for mode -1 (c)parameters for mode 2.

Refractive Index	Mode 1 (nm)	Sensitivity nm/RIU	Mode 2 (nm)	Sensitivity nm/RIU
1.25	456.06	305	559.09	343.4
1.30	464.65	171.8	584.85	515.2
1.35	473.23	171.6	602.02	343.4
1.40	481.82	171.8	619.19	343.4
1.45	498.99	343.6	636.36	343.4

(a)

Refractive index	Sensitivity (nm/RIU)	FWHM (nm)	Accuracy (1/FWHM)	Quality Factor (Sensitivity/FWHM)
1.25	305	76.95	0.012995	3.9636
1.30	171.8	83.55	0.011969	2.0562
1.35	171.6	91.37	0.010944	1.8780
1.40	171.8	96.97	0.010312	1.7716
1.45	343.6	106.95	0.009350	3.2127

(b)

Refractive Index	Sensitivity (nm/RIU)	FWHM(nm)	Accuracy (1/FWHM)	Quality Factor (Sensitivity/FWHM)
1.25	343.4	51.87	0.019278	6.62039
1.30	515.2	48.15	0.020768	10.69989
1.35	343.4	45.81	0.021829	7.496179
1.40	343.4	42.99	0.023261	7.987904
1.45	343.4	44.77	0.022336	7.670314

(c)

From the results, it is seen that as the refractive index of the surrounding medium increases, the biosensor's sensitivity also escalates, indicating that it becomes more responsive to changes in the refractive index. This heightened sensitivity is beneficial for detecting small variations in analyte concentrations or bio molecular interactions. In our designed structure we can see that there are a number of resonances with the strongest SPR at mode1 and mode 2. Moreover, in the transmission spectra of mode1 the SPR is between 430 nm -490nm and for mode 2 the SPR wavelength is between 450-700 nm. Particularly, when the refractive index of the analyte is between 1.30-1.35 the SPR is approximately 584-602 nm the sensitivity is highest, which results 515.2nm/RIU at mode 2 in where the quality factor is also very high of 10.69989. At mode 1 at resonance frequency 498.99nm the highest sensitivity is 343.6nm/RIU where the quality factor is 3.2127.

Grating-based surface plasmon resonance (SPR) biosensors, provides several advantages in terms of simplicity and miniaturization potential, however have a number of limits and obstacles when compared to other SPR biosensors. Grating-based biosensors are often less sensitive, more prone to noise, and have less effective plasmon excitation, resulting in a lower detection limit. On the other hand, fabrication complexity and reproducibility poses considerable challenges because creating high quality grating with precise periodicity and uniformity requires advanced lithography techniques which can be costly and difficult to scale [56]. Additionally, the angular and wavelength range over which gratings can efficiently couple light to plasmons is narrower, limiting the operational flexibility of grating-based sensors for the detection of a wide range of analytes [54].

Multiplexing with dual mode detection could be an intriguing area to focus on in the future. The ability to multiplex the biosensor boosts its efficiency and utility in clinical diagnosis. Implementing similar strategies in a photonic cavity-based biosensor could make it more versatile and practical for biomolecule analysis.

3.6 Application of biosensor in Hb detection

Normal Hemoglobin concentration in blood for females is 12-16g/dl and 14-18g/dl for males but above or below this concentration is very abnormal, it may cause anemia or polycythemia, cancer, heart disease, lung disease, kidney or liver disease [27]. Moreover, postoperative hemorrhages and autologous transfusions can be observed from the Hb level [51]. Hence a suitable amount of Hb must be maintained to ensure adequate oxygenation of the tissue. Generally, the volume of hemoglobin in blood is measured in grams per deciliter (g/dl) or grams per liter (g/l) [51]. In this investigation, the measurement of RIs of the oxygenated Hb concentration could be useful to determine the sensitivity of the designed structure figure 3.6. As there is a slight change in RI due to the concentration of Hb the sensitivity of the transmission vs SPR wavelength can be detected. In 2021, Ajad [51] use a whispering gallery mode (WGM) ring resonator for hemoglobin detection, based on the linear link between hemoglobin concentration and refractive index. Their experiments show that a 0.001 RIU shift in refractive index, there is an associated increase of 6.1025 grams per liter (g/L) in the hemoglobin concentration level. This relationship underscores the significance of monitoring blood refractive index as a potential indicator of hemoglobin concentration [51]. This relationship can be denoted as in equation 3.1 as shown in paper [51].

$$H_r = H_o + B\ \Delta n \qquad (3.1)$$

where H_r is the resultant Hb level, H_0 is the present Hb level, B is the constant value of 5766.5, and the refractive index change is Δn [49].

Performance analysis: The research investigates a range of hemoglobin (Hb) concentrations from 0 to 60 g/dl, simulating diverse blood conditions figure 3.6. The refractive index at the resonant wavelength varies between 1.335 to 1.344 [49] , depending on the specific Hb concentration. Since the surface plasmon resonance occurs at a wavelength of 589.3 nm, the investigation focuses on this wavelength.

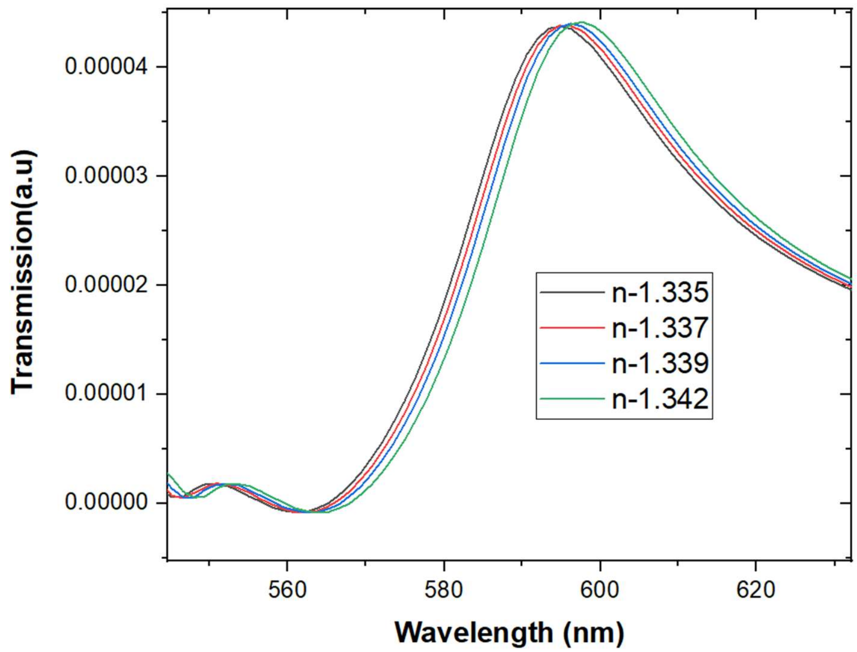

Figure 3.6: Transmittance spectrum with respect to the wavelength for varying Hb concentrations.

A typical human blood hemoglobin levels are between 12-18g/dl but this changes depending on age, sex and health. A level of about 16g/dl is usually seen as normal and healthy. High levels such as 20g/dl or 40g/dl can point to serious blood problems, dehydration or other illnesses and can be bad for one's health. This biosensor can detect the difference between these hemoglobin level changes and is quite sensitive since it can spot normal and abnormal levels. According to the simulation results, when the Hb concentration is very low (0 g/dl), the outcome is 365 nm/RIU. Under healthy conditions with an Hb concentration of 16 g/dl, the sensitivity is 2.5nm/RIU. A high Hb concentration of 20g/dl yields a sensitivity of 355 nm/RIU. This condition can arise in cases of polycythemia, which is a type of blood cancer. And a much higher Hb concentration of 40 g/l, the sensitivity increases to 473 nm/RIU. Table 3.4 demonstrates how this biosensor can detect Hb concentrations at a resolution of 0.001 RI units. However, its performance is not superior to other highly sensitive biosensors. Therefore, we extended our investigation to achieved an improved sensitivity, which has been explained in the following chapter.

Table 3.4: Summary of sensitivity, FWHM, detective accuracy, quality factor and healthy/unhealthy status at varying blood hemoglobin concentration

Sample with varied Hb level (g/dl)	Refractive index	Resonant wavelength (nm) mode 2	Sensitivity nm/RIU	FWHM (nm)	Accuracy (1/FWHM)	Quality Factor	Status
0	1.335	594.825	364.91	45.38	0.02203	8.04	unhealthy
16	1.337	594.830	2.5	45.38	0.02203	0.06	healthy
20	1.339	596.244	354.75	45.18	0.02213	7.85	unhealthy
40	1.342	597.663	472.67	45.10	0.02217	10.48	unhealthy

3.7 Comparison with literature

In paper [55] we can see a two layer grating based sensor using silicon and silicon dioxide. Here, for three-waveguide thickness of silicon layer (220 nm, 150 nm, and 100 nm) the bio-sensing capability is evaluated. It is found that the sensor with a 100 nm thickness provides a higher sensitivity of 322.96 nm/RIU than all other designed structures mentioned in the paper. It has been also assessed that the higher gap width period 440 nm between the gratings has more sensitivity. Compared to the above paper our novel structure has a thickness of 100 nm of silver photonic layer and the gap between the periods is 400 nm which results in the highest sensitivity of 515.2 nm/RIU. This shows that our structure can exhibit better results flexibly than other parametric structures.

Table 3.5 represents the comparison of the obtained results of 2D designed photonic nanoholes cavity structure with other research papers which were also used to detect Hb concentration. Here, we can see that, comparatively, our proposed structure has the best sensitivity over all.

Table 3.5. The comparison of proposed design with recent reported results.

References	Year	Structure	Sensitivity	FWHM
[57]	2019	1 D structure of Air/(SnS/Nanocomposite/SiO_2)/Graphene/D /Graphene/(SnS/Nanocomposite/SiO_2) N/Air. Photonic crystal based with a single defective layer.	51.49nm/RIU	NA
[24]	2020	1D-Photonic crystal cavity based structure is designed by silicon (Si) material.	323 nm/RIU	0.6nm
[58]	2020	A graphene layer of Metal Dielectric Metal configuration nano-scale ring structure.	333 nm/RIU	-
[59]	2019	Sphere, cubic and cylinder shaped silver plasmonic nanoparticles are used to detect Hb concentration blood.	235.7nm/RIU	94 nm
[60]	2022	1D photonic crystal-based sensor using an asymmetric periodic double layers structure of Titanium dioxide TiO_2 and silicon dioxide SiO_2 with a single defect layer.	144.50nm/RIU	
Proposed work	2024	2 D grating structure of nanoholes cavity silver titanium structure (dual mode)	515.2 nm/RIU	48.15nm

The research [60] focuses on a one-dimensional photonic crystal-based sensor using an asymmetric periodic double layers structure of Titanium dioxide TiO_2 and silicon dioxide SiO_2 with a single defect layer, showcasing sensitivity of 144.50 nm/RIU. And also in paper [57] one dimensional ternary photonic crystal with a defective layer is designed for bio sensing. Materials like Graphene, silicon dioxide SiO_2 / Ag and Tin sulfide SnS provide sensitivity 51.49nm/RIU. The research paper [24] focuses on designing a cavity based one-dimensional Photonic Crystal sensor. The sensor design includes alternate silicon layers with introduced porosity to achieve the desired index contrast, enhancing sensing capabilities. The structure demonstrates an average sensitivity of approximately 323 nm/RIU or 0.05 nm/(g/L). Compared to all other biosensors mentioned above where all are mainly detecting Hb in blood, our proposed work has the easiest structure containing nanomaterials silver and titanium only. It is the most available photo activated nanomaterials found and the very cheapest among all the above materials mentioned in other papers. It has a nice analyte chamber which is a nano cavity based hole /grating structure, which helps to interact the analyte with the photonic nanomaterials efficiently. It enhances the electric field's intensity as light travels through the analyte and thin film of titanium and silver photonic metals. As a result, we have the highest sensitivity of 515.2 nm/RIU for which we can detect not only Hb in blood but also other biomolecules.

To conclude, the proposed grating-based Surface Plasmon Resonance (SPR) biosensor offers a novel approach for detecting hemoglobin (Hb) with high sensitivity and specificity [61]. This biosensor leverages the unique properties of surface plasmons oscillations of free electrons at the interface between a metal and a dielectric to monitor changes in refractive index upon Hb binding. The grating structure, which is composed of periodic metallic or dielectric materials, enhances the SPR signal by diffracting incident light to excite surface plasmons more efficiently. This enhancement allows for real-time, label-free detection of Hb at low concentrations, making it suitable for clinical diagnostics and biomedical research. In future, the incorporation of specific antibodies on the grating surface will ensure selective binding of Hb, reducing interference from other proteins. Moreover, the grating-based SPR biosensor offers advantages such as rapid detection times, minimal sample preparation, and the potential for miniaturization and integration into portable devices. This technology represents a significant advancement over traditional Hb detection methods, providing a powerful tool for early diagnosis and monitoring of conditions like anemia and hemoglobinopathies. As research progresses, further optimization of the grating design and functionalization strategies will likely enhance the sensitivity and robustness of this promising bio-sensing platform.

3.8 Fabrication realization

NIL (Nanoimprint Lithography) fabrication is a technique used for creating nanoscale patterns on various substrates. It involves the transfer of a pattern from a mold onto a substrate using a combination of heat and pressure. NIL offers high resolution and high throughput, making it suitable for applications in nanoelectronics, photonics, and biotechnology. The process begins with the fabrication of a mold, which can be made using techniques such as electron beam lithography or nanoimprint lithography itself [62].

Here the spin based mold is then pressed onto the substrate titanium, causing the pattern to be transferred. After the pattern transfer, the mold is removed, leaving behind the desired pattern on the substrate. This biosensor device is made by replicating a pattern using NIL on a resin coated Titanium substrate. Due to its capacity to generate high-resolution patterns, conventional NIL generally uses solid-phase thermoplastic polymers such as polymethylmethacrylate (PMMA) as imprint resins. A high imprint temperature of more than 170° C and pressure of up to 50 bar are required for PMMA resin in order to successfully transfer nanoscale patterns from a stamp mold to the PMMA layer [63]. Using an O_2 plasma etching technique, any excess resin is removed after a 100 nm thick layer of silver is deposited via electron beam evaporation [64]. Here the cavities are 200 nm in diameter and 40 nm in period. The distance between the cavities is maintained at 200 nm in both the vertical and horizontal directions. Cavities are made using the lift off technique in order to remove the resin imprint [63].

NIL can be used to create various types of patterns, including lines, dots, and complex structures. The technique offers advantages such as high resolution, low cost, and compatibility with a wide range of materials. However, challenges such as mold fabrication, alignment, and defect control need to be addressed for widespread adoption of NIL [33]. Figure 3.7 shows the fabrication procedures in steps (copyright © 2017, AIMS Press).

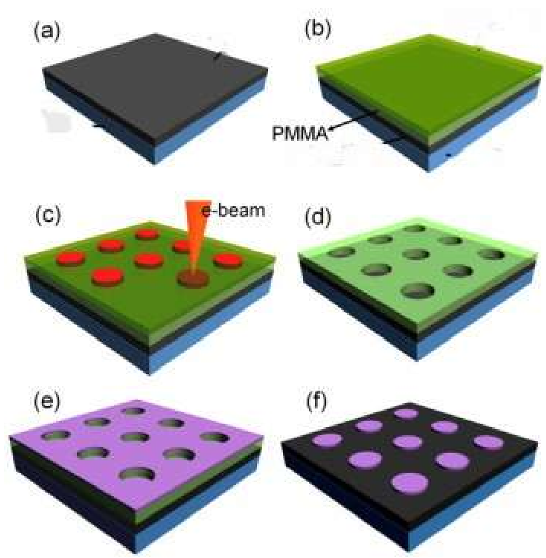

Figure 3.7: Proposed fabrication procedure of the proposed structure a) Titanium substrate b) Spin Resin c) Electron beam lithography d) development e) etching f) lift off [65] (copyright © 2017, AIMS Press).

This two-layered cavity-based system demands high precision to maintain consistent functioning. Acquiring accurate dimensions is technically difficult and necessitates advanced lithography techniques (such as electron-beam lithography) [56]. These procedures are time-consuming and costly [33]. It also requires sophisticated clean rooms and skilled workers to properly handle and manufacture biosensors[56]. Scaling up from laboratory-scale manufacturing to large production while keeping good performance and cheap costs is similarly difficult [66]. While the manufacturing of this is outside the purview of this work, the mentioned fabrication methods may prove helpful for the device's real-time implementation and monitoring, which incorporates mobility [33].

Overall, NIL fabrication is a promising technique for creating nanoscale patterns with high resolution and high throughput, and it has the potential to revolutionize various fields of science and technology.

3.9 Conclusion

We have demonstrated dual mode plasmonic biosensors for SPR mode 1 at 498.99 nm wavelength, sensitivity 343.6 nm/RIU and SPR mode 2 at 585 nm wavelength sensitivity 515.2 nm/RIU respectively. This remarkable sensitivity of our technology offers a promising solution for detecting hemoglobin (Hb) concentration, which is crucial for various medical applications including disease diagnosis and monitoring. Our design is unique which shall be easily fabricated compared to other complex structured configuration models. The biosensor's high accuracy and portability further enhance its utility, enabling rapid and reliable hemoglobin Hb measurements at the point of care. By harnessing the unique properties of nanohole structures this biosensor demonstrates great potential to revolutionize healthcare by providing clinicians with a versatile tool for timely and precise diagnostics. Continued research and innovation in this field hold promise for further improving sensitivity, specificity, and usability, ultimately leading to enhanced medical outcomes and patient care. In this study, we have not obtained blood from any living animals as we performed numerical simulation only.

Chapter 4

MIM - grating based SPR biosensor using metal-Bismuth Selenide (Bi_2Se_3)- Silicon Nitride (Si_3N_4) for multi-analyte detection

4.1 Introduction

This Chapter looks into a new method for creating a Metal –Insulator- Metal MIM grating based SPR biosensor that uses Bismuth Selenide a topological insulator. At first many papers are discussed how other biosensors had some gaps, what are the challenges and how we in our designed biosensor overcame those gaps. Then the material's optical, electrical, anticorrosive and biomedical factors are discussed. The device structure are shown and performed extensive simulation on four different types of configurations. Two optimized structures with better performance were found by altering the dimensions of the Bismuth Selenide gratings. This resulted in a structure highly sensitive to changes in refractive index. By fine tuning the geometrical parameters of nanostructures and the refractive indices of the analytes we developed a biosensor capable of being tuned to detect various biomolecules. After identifying the optimum parameters which have the best performance mosquito borne diseases (dengue and malaria) detection was performed at resonant wavelength between 500 nm-1100 nm, visible light ranges. And for detecting electrolytes and blood glucose, structure 3 was used at high resonant wavelengths between 1900-2500 nm at MIR mid infrared ranges. By using numerical simulations in ANSYS Lumerical FDTD solution 8.19.1584 trial version, sharp resonance was found, achieving sensitivities of 532.36 nm/RIU (Bi_2Se_3-Au-Si_3N_4) and 1035.8 nm/RIU (Bi_2Se_3-Ag-Si_3N_4), surpassing existing on-chip devices. The sensing performance is analyzed through transmission, reflection, FWHM, and quality factor, and demonstrate the biosensor's potential for detecting dengue, malaria, glucose, and electrolytes, offering a multiplexed detection platform suitable for resource-constrained settings. Moreover, the designed structure is compared with other papers and showed how multiplexed designed biosensor with the unique material of Bismuth Selenide, Silicon Nitride has brought novelty to the biosensor industry. Finally, the fabrication process was discussed to be used for real time for implementing and monitoring.

4.2 Material selection

A common material for SPR chips are generally made up of Ag/Au plasmonic materials, a substrate and a thin adhesion layer. Here, our biosensor is based on topological insulator Bismuth selenide, Gold (Au) and Silver (Ag) plasmonic materials and a substrate silicon nitride Si_3N_4. Bismuth selenide Bi_2Se_3 is a material with many sensitivities against various factors, which can be useful in developing biosensors. It crystallizes in a rhombohedral lattice, which helps to promote its unique electronic and thermal properties as a result it is very sensitive to environmental changes [34]. Therefore, Bi_2Se_3 can interact with various biological molecules, which can alter its electrical properties. This sensitivity can be leveraged to develop biosensors that detect changes in conductivity or impedance in response to the binding of target analytes. This substance behaves as an insulator in its bulk but displays distinct electrical states on its surface. Bi_2Se_3 has demonstrated potential for use in photodetectors, modulators, and even as a platform for investigating unusual quantum phenomena in the field of optics. Its layered crystal structure gives it a high refractive index and great optical anisotropy. Bi_2Se_3 is appropriate for infrared applications due to its narrow bandgap and robust photo response over a wide spectrum.

Since it has great optical and electronic properties, it is used for optical sensors that detect changes in light when biological molecules bind to it. It is a three-dimensional topological insulator [67] which realizes high surface-to-volume ratios, which increases the interaction of the biosensor surface with biological molecules for enhanced sensitivity [67]. It is compatible with biological systems [67], which means it doesn't cause harmful reactions when used in medical biosensors, making it safe for detecting diseases . This material is stable under ambient conditions, which is very important for long-term bio-sensing applications. Its chemical and environmental stability means that sensors made with Bi_2Se_3 can be used in various conditions without degradation over time [68].

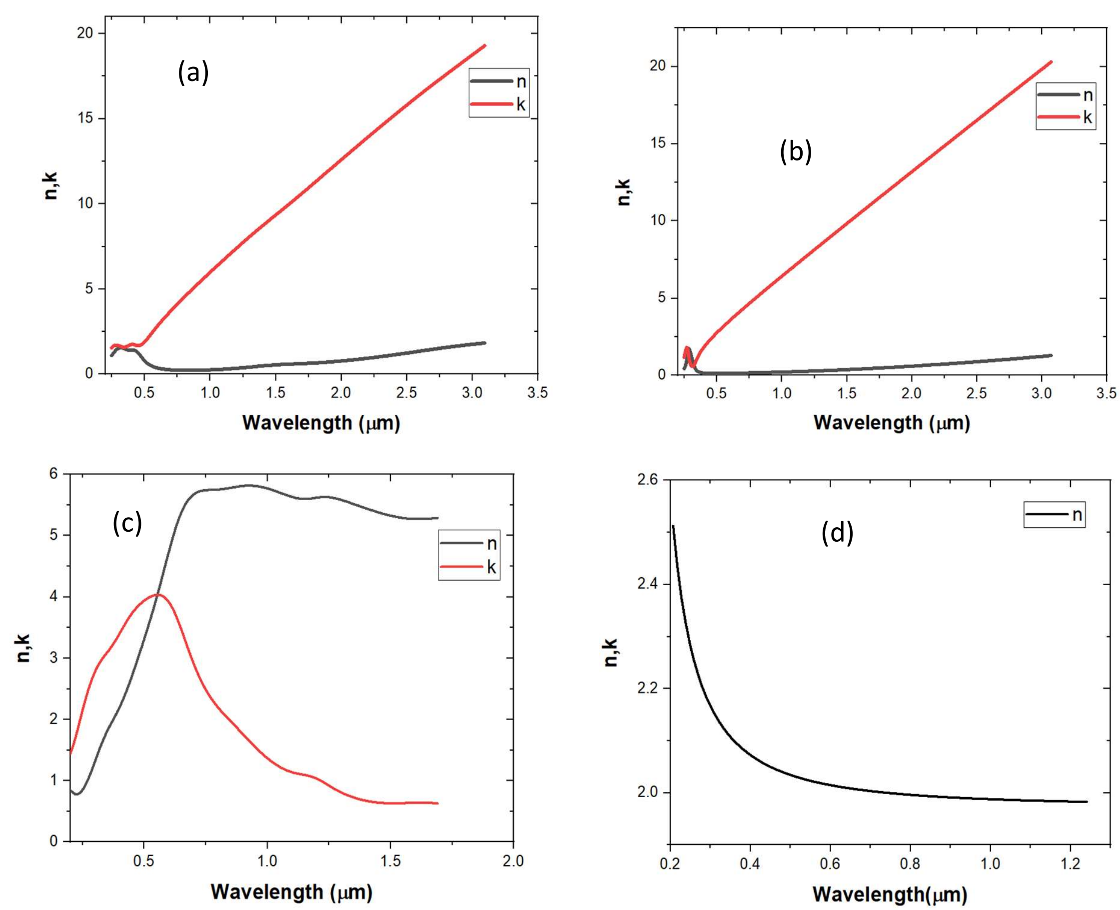

Figure 4.1: Reflective Index (Real/Imaginary) of all materials. a. Gold b. Silver c. Bismuth selenide d. silicon nitride.

Here in figure 4.1 all the materials refractive index is shown with real and imaginary graphs behavior at the best.

In MIM grating based structure, we used both gold and silver as metal layer as a result it had strong surface plasmon resonance when light is illuminated. When this property interacts with electromagnetic waves, it greatly enhances their effectiveness in bio sensing. Gold is resistant to oxidation and corrosion, ensuring longevity in various environments [69]. Silver possesses the highest electrical conductivity of all metals, which enhances its plasmonic response. It supports strong SPR, making it suitable for applications in SERS and optical scattering. Additionally, silver exhibits inherent antimicrobial properties, making it valuable in biomedical applications [70]. Although silver used biosensor achieved highest sensitivity but it has the oxidation properties which brings disadvantages in biosensor.

Silicon nitride (Si_3N_4) is a versatile substrate material composed of high mechanical strength, excellent thermal and low thermal conductivity, making it very suitable for a wide range of applications. It has low optical loss, making it ideal for enhancing the sensitivity of SPR biosensors. The low optical loss means that more light can interact with the surface plasmon waves, resulting in better sensitivity to biomolecular interactions. It is chemically stable and resistant to a wide range of solvents and pH variations, making it ideal for bio-sensing applications that require exposure to different biological and chemical environments [71]. All in all, silicon nitride is transparent in the visible to near-infrared spectrum, hence enabling its use in photonic applications such as waveguides. It is easily functionalized with biological recognition elements like antibodies, DNA, or proteins. This flexibility allows for the creation of highly selective biosensors, enhancing the accuracy and effectiveness of SPR-based biosensors [72]. Because of its hardness, it resists wear and scratch and has exceptional resistance to heat shock. Because of its electrical characteristics, it is used in the field of electronics as a dielectric and an insulator for sophisticated microelectronics applications. It has the ability to withstand chemical corrosion and oxidation also.

4.3 Device structure design

In our study Bismuth selenide is simulated in the form of metal-insulator-metal (MIM) structure. This device embraced MEMS technology which developed a miniaturized device for chemical analysis and diagnostics. Here, figure 4.2 demonstrates the perspective view of the MIM based grating biosensor.

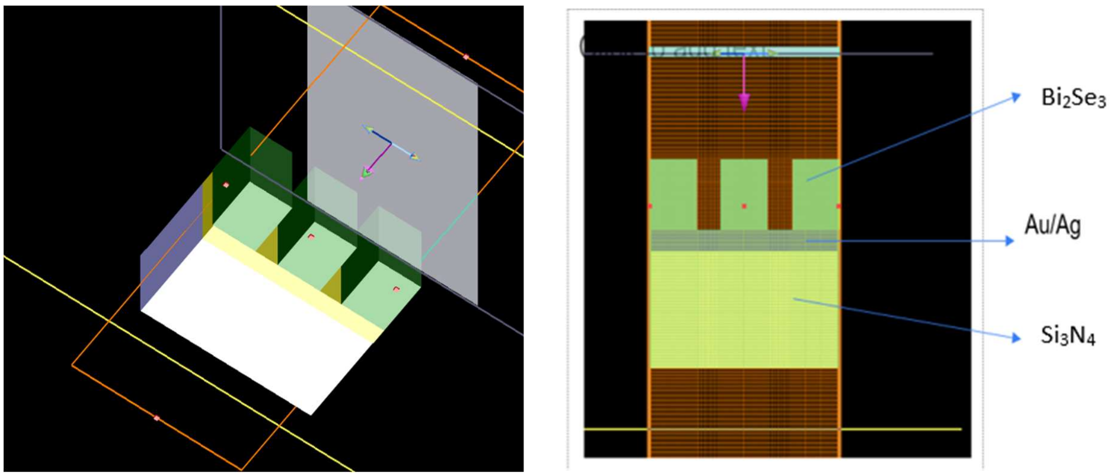

Figure 4.2: Simulation Perspective view (Inset arrow indicates the direction of plane wave and the other arrow shows the direction of TFSF source).

An optical power monitor was placed between the source and lower PML boundaries in order to simulate the optical reflection and transmission data. We used wavelengths at a range from 400 to 3000 nm using the TFSF source. Then after changing the refractive index between 1.25 to 1.50, we examined the sensitivity of the above structure by analyzing the behavior of reflected light. After several investigations when we identified the optimal structure, we found that one of the designs performs best at visible light range with a resonant wavelength between 500-1100 nm and the other structure performs best at MIR Mid infrared range in resonant wavelengths between 1900-2500 nm. We performed the whole simulation using the ANSYS Lumerical FDTD solution 8.19.1584 trial version.

Here in Figure 4.3 shows dielectric-metal grating configuration showing surface plasmon (SP) resonance conditions.

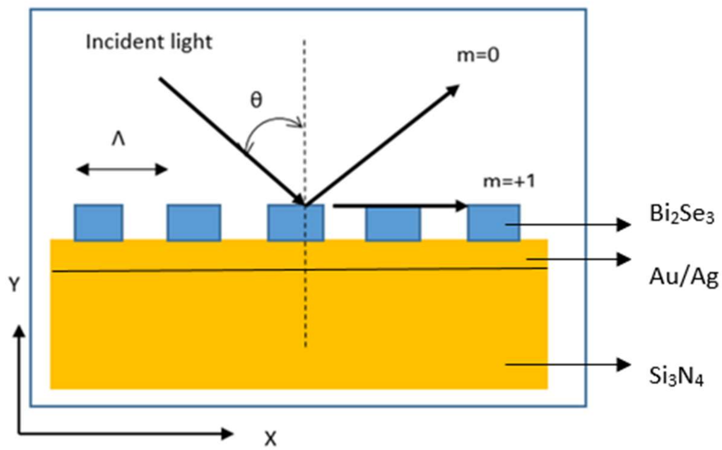

Figure 4.3: Dielectric-metal grating configuration showing surface plasmon (SP) resonance conditions.

4.3.1 Grating structure and its influence on the performance

Periodicity, grating depth, and grating thickness of the periodic gratings are some of the important features which can have a major impact on general sensitivity. As a result, after multiple alterations of the structure's dimensions and parameters we found two designs at which biomolecules can be detected effectively with highest sensitivity. At first we changed the thickness of the middle layer of gold and silver from 50 nm to 120 nm and found out the optimum thickness to get the best outcome as shows the sensitivity of the material on changing thickness of it. Similarly, for silver we identified that the sensitivity is stable between 80 nm to 120 nm thickness. As a result, we concluded that 90nm was the optimum thickness. A thickness of around 90 nm allows for strong coupling of incident light with surface plasmons, maximizing the sensor's sensitivity. At 90 nm, gold and silver allows for an effective propagation of surface plasmons and enhances the sensitivity of the device to minute changes in the refractive index, crucial for bio-sensing applications. Thinner films (<50 nm) reduce the plasmon propagation length and weaken the signal, while thicker films reduce the penetration depth of the evanescent field, limiting the detection zone [73]. Therefore, in both designs we made sure to keep the middle layer constant of width 90nm throughout our investigations. Figure 4.4 shows the sensitivity of gold and silver at different thickness and figure 4.5 shows the 3D schematic of the proposed structure.

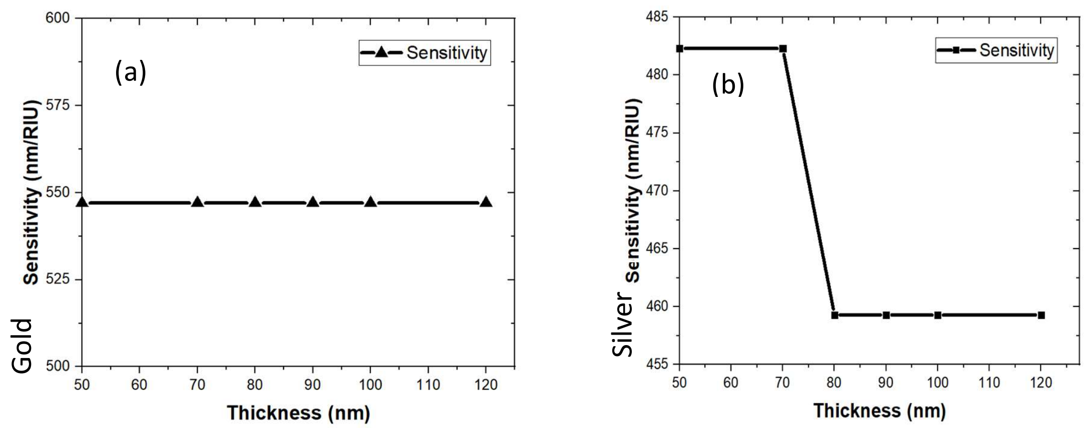

Figure 4.4: Middle layer thickness optimization using gold and silver. Graphs show sensitivity as a function of thickness: a. Sensitivity for the gold thickness of 50 nm,70nm,90nm,100 nm and 120nm. b. Sensitivity for the silver thickness 50nm,70nm,90nm,100 nm and 120nm.

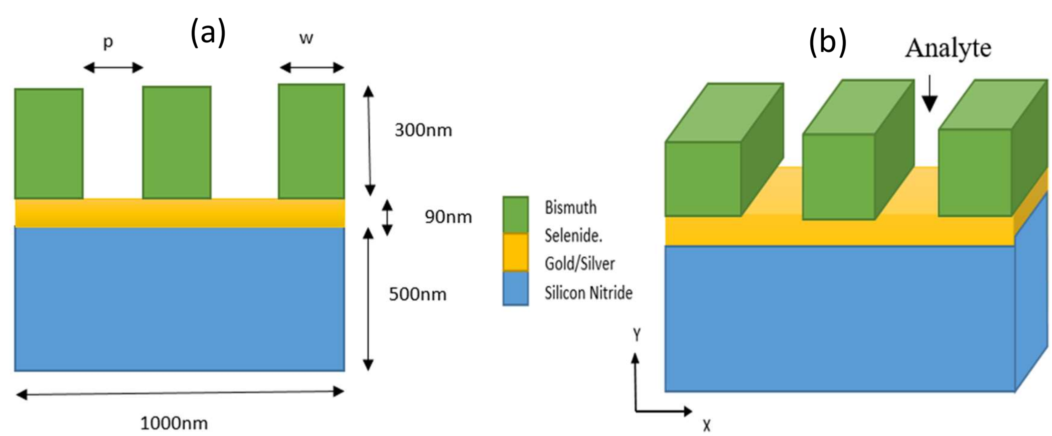

Figure 4.5: a. xy perspective view. b. 3D schematic of the biosensor.

Optimization of top layer Bismuth Selenide: We kept the width and height of all the metal-dielectric layers same as shown in figure 4.5 and designed two structures called design 1 and design 2. In these structures we varied the size of the period and the width of the top layer only. The analyte chamber is marked in the figure 4.5b.

Design 1: In design 1, gold was utilized as the middle layer, while the top layer's period and width were varied across two distinct parameters. Initially, structure 1 (bismuth selenide width-100 nm and period - 400nm) was investigated and the sensitivity was subsequently observed as illustrated in figure 4.6.

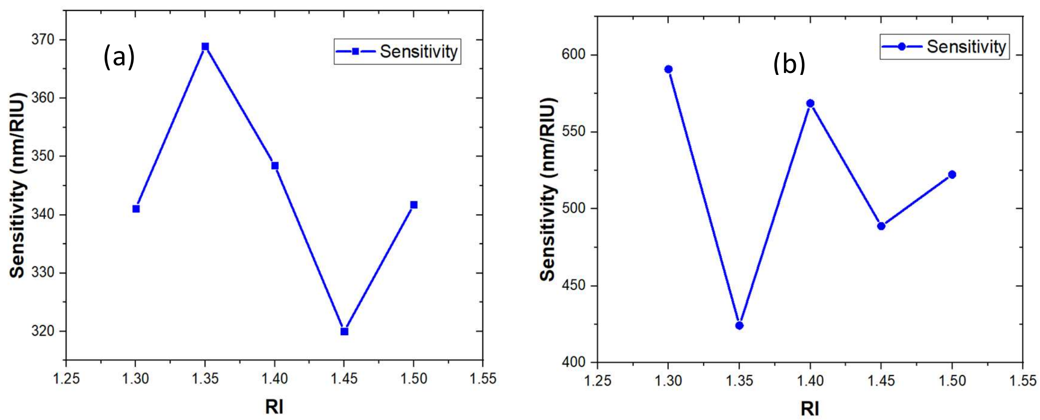

Figure 4.6: Top layer grating structure (height/width/gap) optimization using Bismuth selenide. Both of the graphs show sensitivity as a function of RI. a. Bismuth selenide width-100, period-400. b. Bismuth selenide width-250, period-375

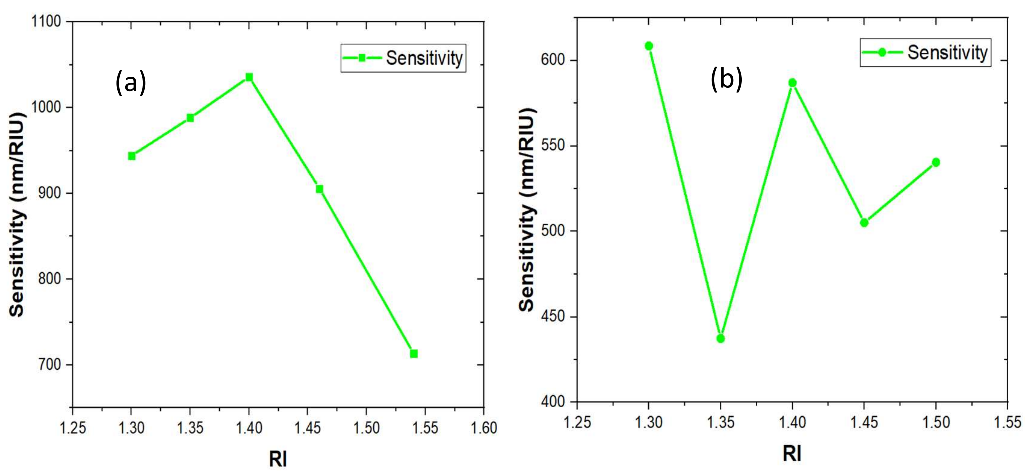

Figure 4.7: Top layer grating structure (height/width/gap) optimization using Bismuth selenide. Both of the graphs show sensitivity as a function of RI. a. Bismuth selenide width-100, period-400. b. Bismuth selenide width-250, period-375.

Following this, structure 2 (bismuth selenide width-250nm, period-375nm) was examined. Figure 4.6 demonstrated that wider strip of bismuth selenide and the smaller grating period of structure 2 lead to maximum sensitivity of 532.36nm/RIU. Conversely structure 1, with its relatively smaller width and larger grating period exhibits a lower sensitivity of only 368.94nm/RIU.

Design 2: In design 2, a silver middle layer was utilized and two structures were explored by varying the grating periodicity and width of the top bismuth selenide layer. Figure 4.7, illustrates that for each structures the sensitivity changes on different refractive index. The highest sensitivity of 1035.8nm/RIU is achieved from structure 3 (bismuth selenide width-100 nm, period-400nm.) while structure 4 (bismuth selenide width-250 nm, period-375 nm) exhibited comparatively lower sensitivity of 608.52nm/RIU.

4.4 Performance analysis of optimum structure

In advance, by detecting the sensitivity of their distinct structures we have decided the optimum structure which performs best as a biosensor to detect analytes. For detecting dengue, malaria, blood glucose and electrolytes, we decided to keep the source light of wavelengths between 400-3000 nm. Due to the strong localization of electromagnetic fields at metal insulator junctions, the MIM based RI sensor's performance metrics are extremely sensitive to structural parameters. Therefore, for optimal performance structural parameters must be fine-tuned.

As a result, we had exploited the following sequential optimization and concluded that Structure 2 where the top layer bismuth selenide parameters of (Width-250 nm, Period-375 nm) and middle layer gold (Au) has the best sensitivity of 532.36nm/RIU. And the structure 3 where for the top layer bismuth selenide parameters of (Width-100 nm, Period-400nm) and middle layer silver (Ag) has the best sensitivity of 1035.8nm/RIU. Here mainly the parameters of the period and width of bismuth selenides affected the sensitivity.

Through our series of investigations to determine the optimal parameters, we found that when using gold, the insulator Bismuth selenide with a small width of w=100 nm in design 1 exhibited lower sensitivity compared to design 2. Additionally, when silver was used, the sensitivity varied significantly with the Bismuth selenide width. Specifically, structure 3, featuring a smaller width of w=100 nm period =400 nm demonstrated higher sensitivity than structure 4, which had a width of w=250 nm period =375nm. These findings clearly indicate that the width of the grating material plays a critical role in influencing the sensitivity characteristics of the biosensors. According to paper [74] it has been reported that wider gaps in silver plasmonic material play a significant role in efficiently coupling incident light to plasmon modes. This leads to increased excitation in areas with larger gaps. Furthermore, for different gap widths a more complex plasmonic response is produced compared to uniform grating designs. Additionally, we have observed that silver has lower real dielectric constant than gold, which results in a higher coupling efficiency between light and surface plasmons.

From the paper [75], it was observed that when the grating period is 400 nm, silver material provides higher sensitivity compared to gold, despite its larger period gap. Therefore, structure 3 achieves highest sensitivity compared to structure 4. In contrast, in design 1 where gold plasmonic material was used, it exhibits optimal sensitivity at smaller grating periods. For instance, structure 2 with a period of 375nm shows better performance compared to structure 1.

Below table 4.1 summarizes the structural parameters of each design.

Table 4.1: Dimension and material optimization with sensitivity and operating wavelength

Proposed structures	**Top layer**	**Middle layer**	**Sensitivity (nm/RIU)**	**Operating wavelength(nm)**
1st:Bi_2Se_3-Au-Si_3N_4	Gold	Bismuth selenide, Height-300 nm,Width-100 nm, Period-400nm	368.94	500-800
2nd: Bi_2Se_3-Au-Si_3N_4	Gold	Bismuth selenide, Height-300 nm,Width-250 nm, Period-375 nm	532.36	500-800
3rd: Bi_2Se_3-Ag-Si_3N_4	Silver	Bismuth selenide, Height-300 nm,Width-100 nm, Period-400nm	1035.8	1900-2400
4th: Bi_2Se_3-Ag-Si_3N_4	Silver	Bismuth selenide, Height-300 nm,Width-250 nm, Period-375 nm	608.52	900-2400

After identifying the optimum parameters which have the best performance we identified that for dengue and malaria detection, we used structure 2 as it has the best resonant wavelength between 500 nm-1100 nm at visible light ranges. And for detecting electrolytes and blood glucose, we decided to use structure 3 as it performs finest at high resonant wavelengths between 1900-2500 nm at MIR mid infrared ranges. Below the figure 4.8 shows the reflectance spectra versus wavelength of structure 2 and 3.

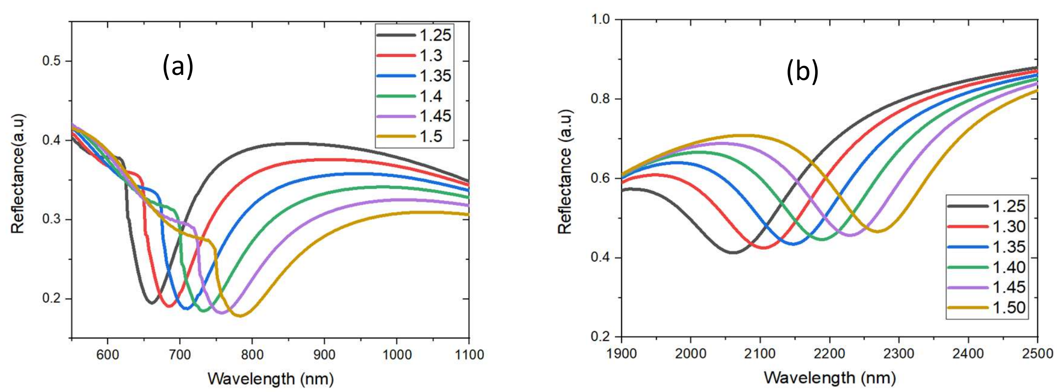

Figure 4.8: a. Reflectance versus wavelength for **structure 2**. b. Reflectance versus wavelength for **structure 3**

The sensitivity and other performance outcomes of structure 2 and 3 are shown in table 4.2.

Table 4.2: a. Performance parameter for structure 2 and b. Performance parameter for structure 3

RI	Resonant Wavelength peak 1(nm)	Sensitivity (nm/RIU)	FWHM (nm)	Detection accuracy (1/FWHM)	Quality Factor (Sensitivity/ FWHM)
1.25	661.329	-	70.49235	0.0141859	-
1.30	683.635	446.12	75.49323	0.0132462	5.909
1.35	710.253	532.36	76.98142	0.0129901	6.915
1.40	733.088	456.7	82.17304	0.0121694	5.558
1.45	757.439	487.02	93.98721	0.0106397	5.182
1.50	783.465	520.52	95.60927	0.0104592	5.444

[a]

RI	Resonant Wavelength (nm)	Sensitivity (nm/RIU)	FWHM (nm)	Detection accuracy (1/FWHM)	Quality Factor (Sensitivity/FWHM)
1.25	2058.62	-	151.89	0.006583	-
1.30	2105.82	944	178.54	0.005600	5.287
1.35	2155.23	988.2	180.22	0.005548	5.483
1.40	2207.02	1035.8	184.84	0.005410	5.603
1.46	2261.36	905.6	187.61	0.005330	4.827
1.54	2318.45	713.6	152.80	0.006544	4.670

[b]

4.5 Application of dual mode biosensor

Our proposed MIM grating based structure presents possible uses in the identification and diagnosis of dengue and malaria infections. From the above sensitivity table 4.2 and reflectance verses wavelength graph we can recognize that the biosensor chip we proposed is able to diagnose the patient with dengue virus.

4.5.1 Detection of dengue and malaria

Dengue fever is a viral illness spread by mosquito bites. This virus which mosquitoes spread while biting is known as Dengue virus (DENV). There are four different types of Dengue virus: **DENV-1**, **DENV-2**, **DENV-3**, and **DENV-4 [76]**. If someone gets infected with one type, they usually won't get that same type again, but they can still catch the other three. This means a person can have dengue up to four times, once of each type. The main mosquitoes that spread dengue are *Aedes aegypti* and *Aedes albopictus* [77] . In recent years we have seen a big rise in dengue infection in tropical areas.

The initial symptoms and signs are relatively mild and include things such as fever and headache. However, it can develop into the fatal disease dengue hemorrhagic fever (DHF) [78]. Right now, there's no specific treatment or vaccine for dengue that's why detecting the infection early is really important [79]. There are several ways to diagnose it, but our MIM grating structure-based biosensors provide a quick and easy method to detect the virus right away, which could speed up diagnosis. We look at the refractive index of a blood sample, which contains hemoglobin, platelets, and plasma, to check for the dengue virus [79]. Notably, changes in hemoglobin levels in the blood plasma could be an important sign for identifying dengue early [77].

Malaria is the most widespread illness in tropical and subtropical areas. It's caused by tiny parasites called Plasmodium, which are spread through bites from female Anopheles mosquitoes [80]. The deadliest type of malaria comes from Plasmodium falciparum, and it damages red blood cells [77]. These parasites deteriorate the healthy RBC and make it infectious [81].

4.5.2 Detection of dengue NS1 antigen

As for detecting the dengue virus, we looked at the thickness of blood samples and checked the refractive indices of infected plasma, platelets, and hemoglobin. This helps in identifying dengue virus quickly, which is important for early treatment. Our biosensor can easily identify the infected plasma and detect the infection. The changes in the resonance wavelength shift makes it possible to identify dengue in that sample. Infected blood samples are crucial for picking up the virus early, often showing up from day one of the infection. Usually, in the first week of infection, the virus level in blood ranges from 0.04 to 2 μg/mL but can spike to 50 μg/mL sometimes. We noticed that the refractive index values for this situation lean towards 1.348 to 1.350 [77]. The recorded RI values, ranging from 1.348 to 1.350, indicate a slight fluctuation in the refractive index by approximately 10^{-3} [35]. This small change in the Refractive index is significant enough to produce noticeable wavelength when measured with our specialized biosensor [82]. Table 4.3 provides a comparison of the RI measurements for normal and dengue-infected blood components. Detection of the dengue virus can be achieved by observing changes in the resonance wavelengths of blood components between healthy and infected blood cell. In table 4.3 shows the variations in wavelengths for healthy and sick individuals regarding hemoglobin, platelets, and plasma. In 2023, there were over 6.5 million reported dengue cases worldwide, along with more than 7,300 deaths across 80 countries, making it the highest number of dengue cases ever reported. Brazil saw more than 4.5 million of those cases and 2,300 deaths, while Asian nations like Bangladesh, Thailand, and Vietnam also reported high case numbers, with Bangladesh alone at 321,000 cases [83].

The number of dengue cases in Bangladesh has increased substantially in recent years. In the 2019 outbreak, for instance, there were more than 100,000 cases with over 160 recorded deaths. On average, Bangladesh has witnessed several thousand confirmed cases of dengue each year since 2000, with spikes during major outbreaks [83]. Table 4.3 illustrates the diagnosis of dengue infection and figure 4.9 shows the reflection spectra of normal and infected plasma, hemoglobin and platelets.

Table 4.3: Diagnosis of Dengue infection.

Blood component	Stage	Refractive Index	Resonant wavelength (nm)	Sensitivity (nm/RIU)
Plasma	Normal plasma	1.350	710.253	-
	Infected plasma	1.337	702.053	630.769
Hemoglobin	Normal hemoglobin	1.390	727.243	-
	Infected hemoglobin	1.357	710.253	514.848
Platelet	Normal platelet	1.365	715.827	-
	Infected platelet	1.400	733.088	493.171

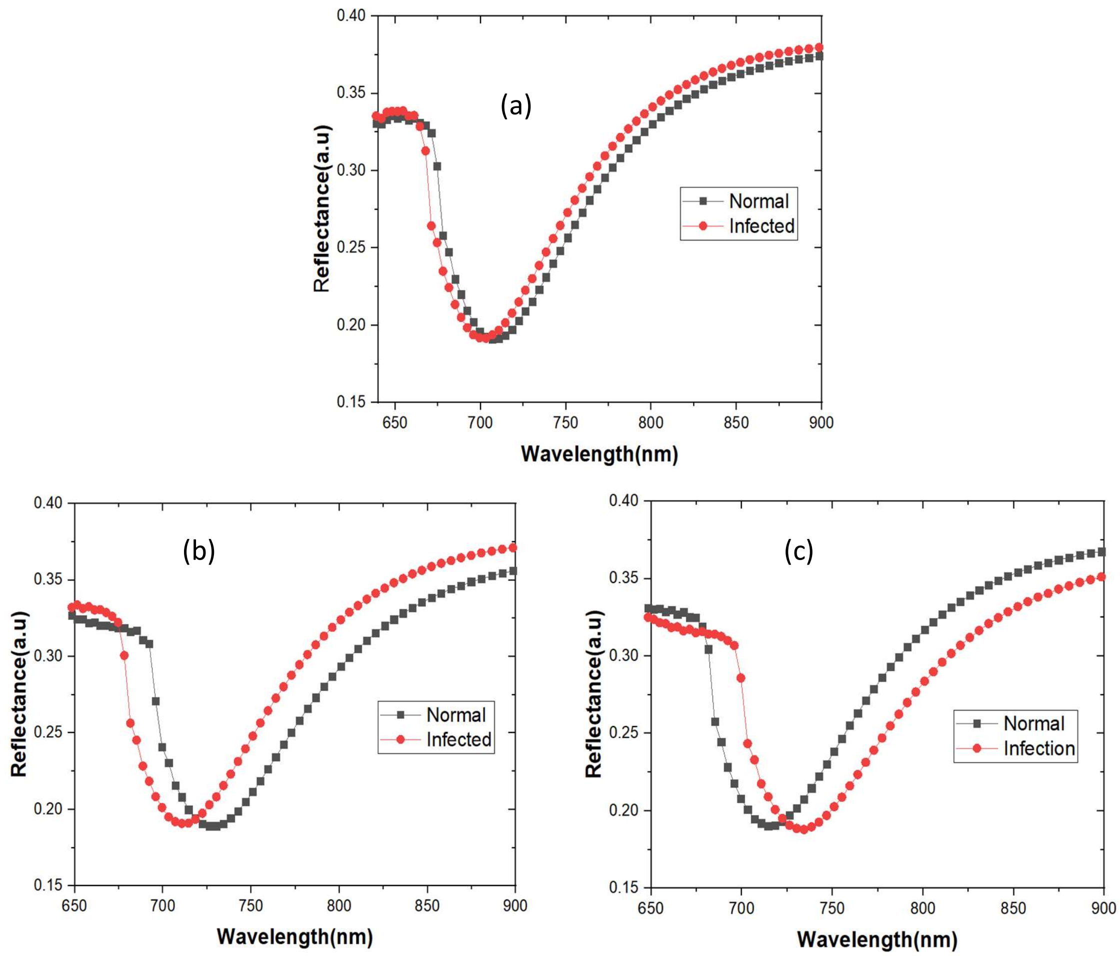

Figure 4.9: a) Reflection spectra of normal and infected Plasma b) Reflection spectra of normal and infected Hemoglobin and c) Reflection spectra of normal and infected Platelet.

4.5.3 Detection of malaria infected RBC

More than 500 million people are impacted from malaria each year, which results in one to two million deaths. Approximately 5,000 confirmed malaria cases and around 50 to 100 deaths are reported annually in Bangladesh, though fluctuations occur based on control efforts and environmental conditions [84].

The host's red blood cells (RBCs) are severely impacted by the parasite. It develops inside the RBC and absorbs nutrients from the RBC's cytoplasm as well as other extracellular elements [85]. When parasites consume plasma Ca^{2+} ions, it triggers blood clotting, leading to inflammation and other issues [86]. Malaria can cause serious problems like jaundice, quick loss of red blood cells, kidney failure, seizures, coma, and even death. Infected red blood cells go through three stages: the trophozoite stage lasts 24 to 36 hours, the ring stage lasts about 24 hours, and the schizont stage takes 40 to 48 hours [77]. Malaria affects the red blood cell refractive index because it changes the hemoglobin levels and how uniform the cells are, which alters how they interact with light. The refractive index values we get from measuring infected blood range from 1.373 to 1.402 [77].

The resonance wavelength of the infected malaria RBCs was compared to sample blood from patients. At first separate RBCs from the blood sample, after that we put the remaining RBC sample onto the MIM biosensor design. The interactions between malaria-affected RBCs and the resulting shift of resonant wavelength indicated in the table are compared to diagnose malaria on the provided blood sample. You can see how the sensor responds to RBCs at different stages of malaria in the provided figure 4.10, which shows the reflectance spectra.

Below table 4.4 clarifies the response of the sensor on different stages of malaria infected RBC.

Table 4.4: Diagnosis of malaria infected RBC

Stages of Malaria infected red blood cells.	Refractive index	Resonant Wavelength (nm)	Sensitivity (nm/RIU)
Normal stage	1.402	733.088	-
Ring stage	1.395	730.153	419.29
Trophozoite stage	1.383	727.243	242.5
Schizont stage	1.373	718.647	859.6

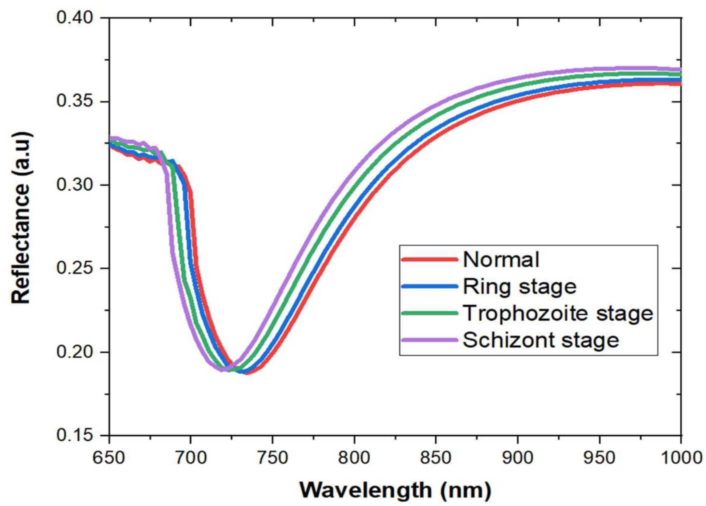

Figure 4.10: Reflectance spectra for different stages of Malaria

4.5.4 Detection of blood electrolytes and glucose

Electrolytes, charged molecular species in the human body, play a crucial role in regulating cellular activity and the function of various organ systems through the coordinated actions of hormones and neurons. An imbalance in electrolytes, whether a deficiency or surplus—particularly of sodium (Na^+), the primary extracellular cation, and potassium (K^+), the main intracellular ion [87]. It can have severe consequences, including life-threatening cardiac rhythm abnormalities. For patients with diabetes, monitoring electrolyte levels is especially important, as insulin regulation is closely linked to both blood glucose and potassium balance. In this study, the sensor's performance was tested by filling its cavities with varying concentrations of Na^+, K^+ and glucose solutions after optimizing its structure.In table 4.5 it is shown that at different concentrations of glucose and electrolytes it has varying RI. For 200 to 440 mg/dL of Na^+ solution the RI ranges from 1.3602 to 1.3874, for 0 to 80 mg/dL K^+ solution the RI ranges from 1.3329 to 1.3450 and for 110 to 230 mg/dL glucose solution the RI ranges from 1.4631 to 1.6058 [88]. The reflectance curves showed distinct peaks that varied with the solution concentrations. To analyze and differentiate these reflectance curves, the refractive index values of Na^+, K^+, and glucose solutions, corresponding to typical blood concentration ranges, were utilized [89]. Our novel MIM-based biosensors structure is able to quantify the concentration of unidentified human blood samples because it has the capacity to integrate at the nanoscale with high efficiency [88].

Table 4.5: Resonant wavelength of blood glucose and electrolytes.

Electrolyte	mmol/L	mg/dL	Refractive Index	Resonant wavelength(nm)	Sensitivity (nm/RIU)
Glucose	6.11	110	1.4631	2240.12	-
	7.78	140	1.4988	2266.01	725.21
	9.44	170	1.5344	2296.98	869.94
	11.1	200	1.5701	2324.22	763.03
	12.8	230	1.6058	2352.1	780.95
Na^+	86.95	200	1.3602	2153.98	-
	113.0	260	1.3674	2161.9	1100
	139.1	320	1.3743	2165.88	576.81
	165.2	380	1.3810	2173.88	1194.02
	191.3	440	1.3874	2177.91	629.69
K^+	0	0	1.3329	2131.71	-
	5	20	1.3360	2135.17	1116.13
	10	40	1.3390	2137.48	770
	15	60	1.3420	2139.79	770
	20	80	1.3450	2142.11	773.33

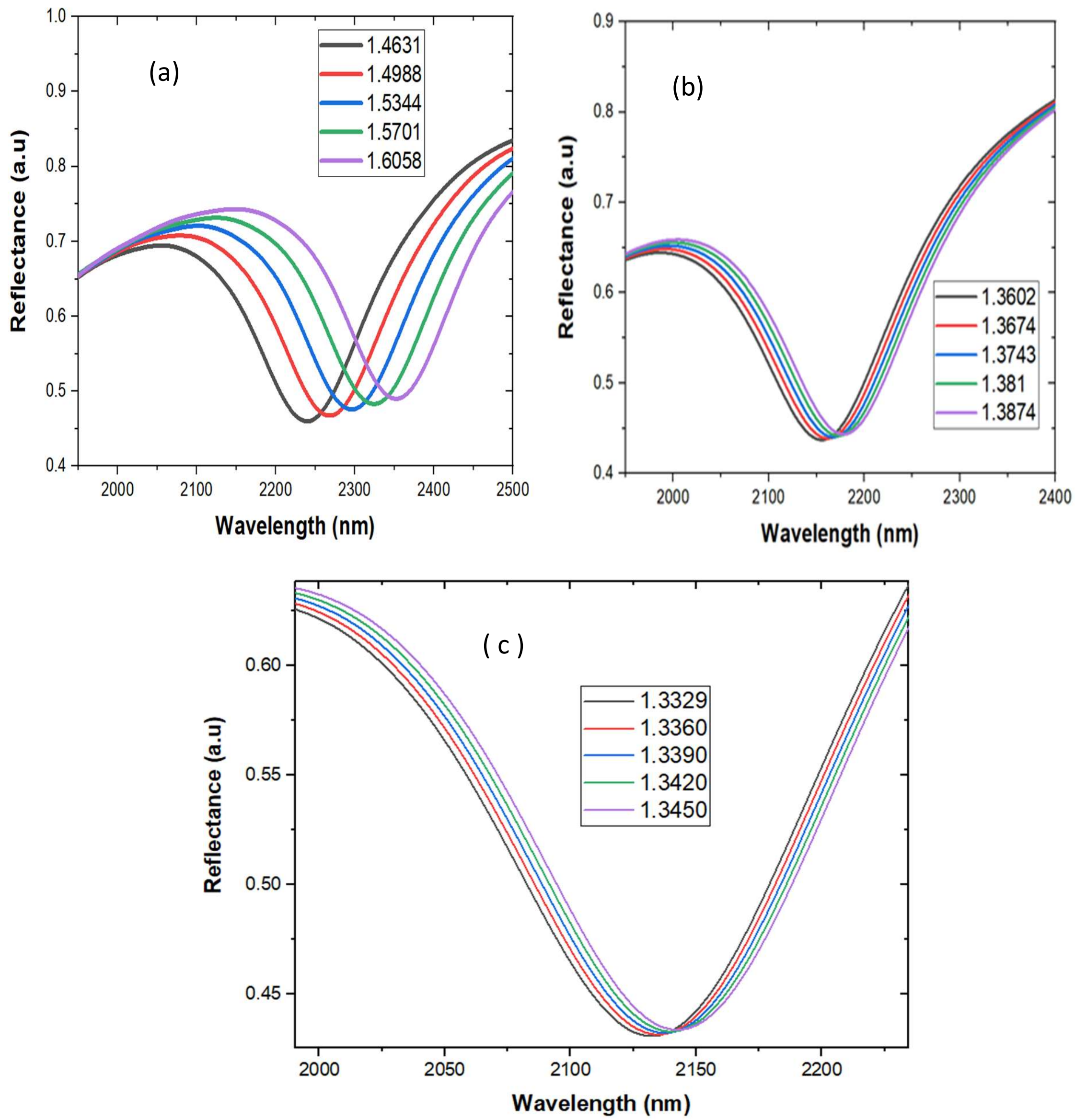

Figure 4.11: Reflectance vs. Wavelength at optimized structural setup (a) 110 to 230 mg/dL glucose solution. (b)) 200 to 440 mg/dL Na^+ solution. (c) 0 to 80 mg/dL K^+ solution.

From Table 4.5 we can assess that the sensitivity range of glucose detection is 725.21-869.94 nm/RIU, the sensitivity difference is almost 145nm/RIU. Its sensitivity variation percentage is moderate within a close range of 7% from mean sensitivity. It has good repeatability, as each RI intervals produced more or less similar sensitivities. For potassium detection, we can observe that it has moderate sensitivity range from 770-1116.13 nm/RIU, the sensitivity variation percentage is almost 17% from mean sensitivity. We observed that on increasing refractive index it has stable output and on same refractive index change it has identical sensitivity. Finally, for sodium detection the sensitivity range is highest, it's between 576.81-1194.02 nm/RIU. Here we detected a sensitivity spike in between 1.3743-1.3810 RI, which may probably due to resonance effect and that give rise to sensitivity variation to 31%.

4.6 Comparison

The research BMH Kumar [90] focused on a two-dimensional structure which is used to detect malaria. In this study, it shows two layers: the sensing portion is at the top, and the base layer supports the sensor. The base material is silicon dioxide, while the sensing component is composed of holes in the silicon layer. Defects happen when there aren't enough Z-shaped holes in the sensor array from start to finish. To adjust the resonance point, a defective point is added to the center line, making it sensitive at 225 nm/RIU. Another study [91] talks about a biosensor for malaria that's made from a 1D faulty photonic crystal. It has a defect layer placed between silicon and lanthanum flint. This biosensor achieved a sensitivity of 327.7 nm/RIU. In the comparison table we tried to bring other papers which detected dengue, blood glucose and blood electrolytes also. For example, a biosensor by B Mohapatra [92] can detect the Dengue virus with a sensitivity of 300 nm/RIU using a 1D photonic crystal design that includes silicon along with LiF and MgF materials. For detecting blood glucose, a research [26] is done where the biosensor is made of 1D photonic crystal of silicon and silicon dioxide. It has the sensitivity of 206.3nm/RIU only. Another research paper [93] where 2D photonic crystal biosensor is designed as an X shaped ring resonator using graphene oxide has sensitivity of 300 nm/RIU . The mentioned biosensors above in the table have several limitations, among them are materials availability and stability. On the contrary, our proposed structure is comparatively easily fabricated and materials are available. Moreover, Bismuth selenide material's optoelectronics properties made the structure more unique and innovative than other designed structures.

Table 4.6 represents the comparison of the obtained results of 2D designed photonic MIM based grating structure with other research papers which were also used to detect dengue, malaria, blood electrolytes and blood glucose concentration. Here, it is evident that comparatively our suggested structure has the best sensitivity from others.

Table 4.6: Comparison with literature

References	**Year**	**Detection**	**Material**	**Sensitivity (nm/RIU)**	**FWHM (nm)**
[90]	2021	Malaria	SiO2 substrate, Si slab with air holes	225	-
[91]	2023	Malaria	Si and lanthanum flint material	327.7	-
[92]	2022	Dengue	Design comprises Si with LiF and MgF materials.	300	-
[26]	2023	Blood glucose	Si and Silicon dioxide	206.3	-
[93]	2022	Blood Electrolytes	Graphene oxide	375	-
Proposed work	2025	Design 1- Dengue, Malaria	Gold and Bismuth selenide	532.36	76.98142
Proposed work	2025	Design-2 Electrolytes and blood glucose	Silver and Bismuth selenide	1035.8	184.84

4.7 Fabrication Realization

A method for producing nanoscale patterns on a variety of substrates is called NIL (Nanoimprint Lithography) fabrication [61]. It requires applying pressure and heat to transfer a pattern from a mold onto a substrate. Because of its high resolution and high throughput, NIL can be used in photonics, biotechnology, and nano electronics. The first step in the process is creating a mold, which can be done with methods like electron beam lithography or nanoimprint lithography [62].

Here, the spin-based mold gets pressed onto the Silver Nitride substrate to transfer the pattern. Once that's done they take the mold off, leaving behind the pattern on the substrate. This biosensor device uses Nanoimprint Lithography NIL to copy a pattern/ design onto a resin-coated Silver Nitride substrate. High resolution designs are often made using solid phase thermoplastic polymers like PMMA polymethylmethacrylate because they work well as imprint resins in traditional NIL. To effectively imprint nanoscale designs from a stamp mold onto the PMMA layer, PMMA resin needs to be at high temperature, over 170°C and under a pressure of 50 bar [63].

After applying a 300 nm thick film of Bismuth selenide using electron beam evaporation, excess resin gets cleaned up with an O_2 plasma etching method [64]. The width and period of the gratings are adjusted based on what the experiment requirements. And then the gratings are made using a lift-off process to get rid of the resin stamp. With NIL, you can create all sorts of patterns like lines, dots, and complex shapes. This method is cheap, works with different materials, and offers high resolution but has some challenges that need fixing before it can be more widely used. Issues like mold making, alignment, and controlling defects need to be sorted out. For a MIM grating system to work well, it needs to be made with a lot of precision [56].

Getting the right dimensions can be tough due to technical challenges and the advanced techniques required, like electron beam lithography, which can take a lot of time and money.

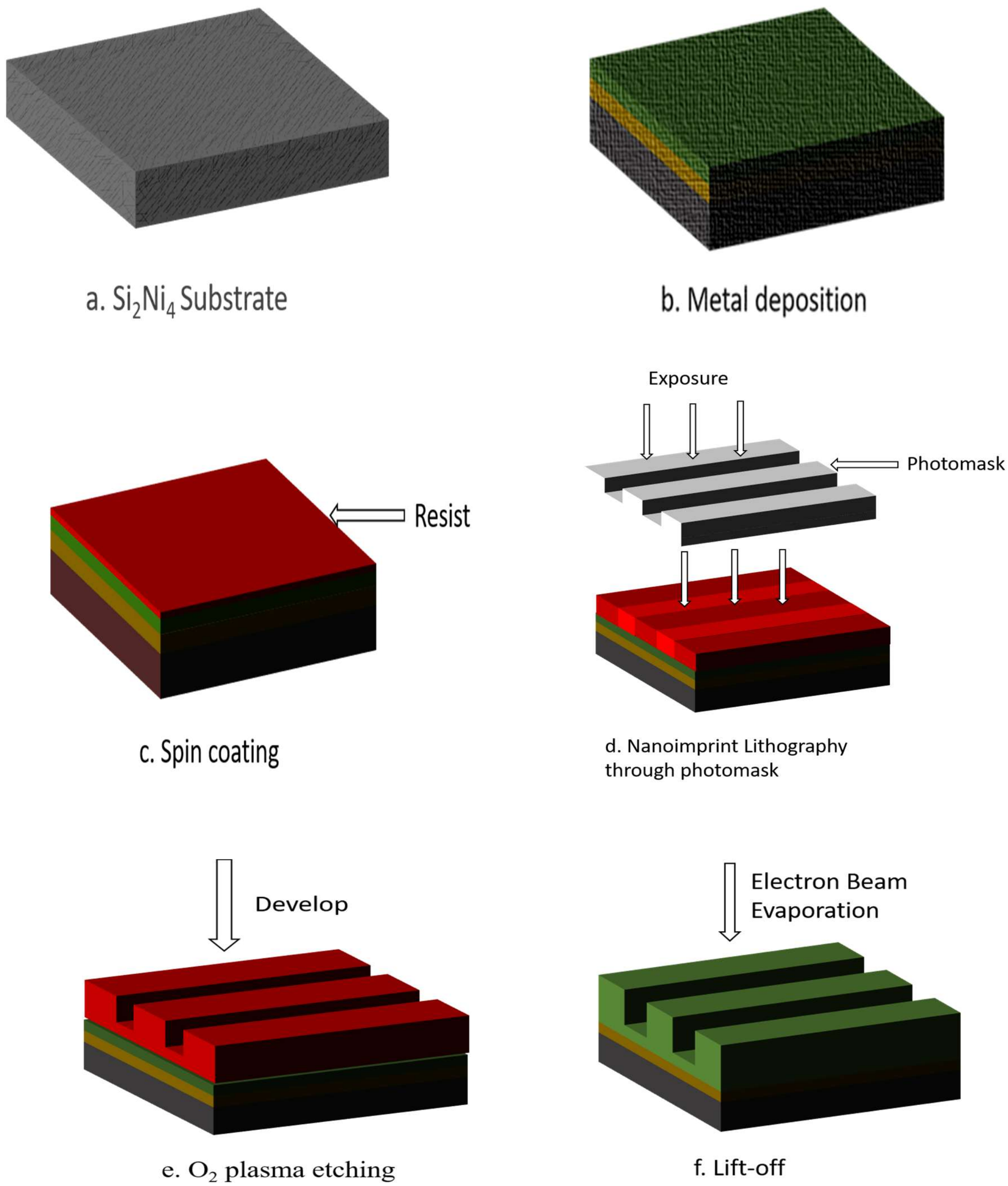

Figure 4.12: Fabrication process of proposed MIM grating based sensor.

In addition, running biosensors needs skilled people and specialized cleanroom setups. Another challenge is making things in the lab to mass production while still keeping quality up and costs down. This work isn't fully detailed for manufacturing, but the methods mentioned could be easily used for real-time implementation and monitoring. Figure 4.12 displays the fabrication procedures in steps.

4.8 Conclusion

In conclusion, we present a SPR-based MIM-grating biosensor, achieving sensitivities of 532.36 nm/RIU and 1035.8 nm/RIU. This represents a significant advancement in biomolecular detection as the structure features a dielectric-metal-dielectric tri layer architecture incorporating Bismuth Selenide- Gold/Silver- Silver Nitride arrangement. The inclusion of Bismuth Selenide introduces a novel element to the biosensor industry due to its optoelectronics characteristics. The design enables sensing and detection across the visible light range and MIR range. Initially, we detailed the underlying mechanism that drive the high performance characteristics of the structure. Furthermore, we analyzed how variations in structural parameters influence sensitivity. The biosensor successfully demonstrated detection of dengue, malaria, glucose and electrolytes. Despite limitations in bulk fabrication, the structure's clear design and simplicity make it an excellent candidate for various applications including point of care, clinical laboratories, blood transfusion services and disaster relief operations. Further development will enhance its capabilities, this technology can be adapted into wearable or implantable devices for chronic disease management and post-operative care.

Chapter 5

Conclusion and future prospect

5.1 Conclusion

In this study we developed three new MIM based SPR structures. In chapter 3 we used silver and titanium materials where the structure is nanohole array integrated and in Chapter 4 we designed two separate structures composed of Bismuth selenide, gold, silver nitrate and bismuth selenide, silver and silver nitrate in a grating based structure. The optimized structure analyzed in chapter 3 is suitable for developing dual mode SPR in the visible light range which enables effective sensing of both bulk refractive index changes and low concentration analytes. As a result, we can detect the hemoglobin concentration in blood at the lowest level. In chapter 4, from the optimized two structures we achieved sensitivity of 532.36 nm/RIU from Bi_2Se_3-Au- Si_3N_4 structure and sensitivity of 1035.8 nm/RIU from Bi_2Se_3-Ag- Si_3N_4 structure. This research shows the variations in wavelength bandwidth due to the variations of resonant structure. We have also compared the results and optimized structure with recent related grating based MIM structures. The incorporation of Bismuth selenide in the structure makes the structure more innovative compared to traditional plasmonic materials. Numerical results show that the suggested reflectance has made the detection of mosquito borne diseases easy. Moreover, blood electrolytes and blood glucose can also be detected using this miniature device.

5.2 Summary of this thesis

Chapter 1 reviewed literatures of different structural types of surface plasmon resonance. Then their gaps and challenges were examined. Next, chapter 2 presented the theoretical analysis of

SPR. Chapter 3 detailed our initial study where a grating-based Surface Plasmon Resonance (SPR) optical biosensor was designed made with silver and titanium. The goal is to make it sensitive and easy to produce. The sensor works by spotting changes in the refractive index of its surroundings through shifts in resonance wavelength. Using the Finite-Difference Time-Domain (FDTD) method for simulations showed clear SPR peaks in the 450–700 nm range. The device is really sensitive, responding with 343.6 nm/RIU at 498.99 nm (mode 1) and 515 nm/RIU at 585 nm (mode 2), which is better than many other on-chip SPR biosensors.

The study also compares important performance factors like transmission, reflection, full width at half maximum (FWHM), and quality factor to judge how well it detects things. Moreover, the sensor was tested for hemoglobin in blood, showing it can work well for a variety of biomolecules like proteins, glucose, fructose, nucleic acids, and cells. These findings point to the sensor being a solid choice for compact and accurate biomedical tests.

Then in chapter 4 our second study that uses a Metal-Insulator-Metal (MIM) setup made with gold/silver, silicon nitride, and bismuth selenide is discussed. It’s built to tackle issues with sensitivity and complexity that come with traditional SPR sensors, allowing the tuning of resonance wavelengths just by changing the sizes and thicknesses of the materials. Using numerical simulations, the results show clear resonance peaks in the visible light range of 450 to 800 nm. The sensor shows impressive sensitivity to refractive index changes, with values of 532.36 nm/RIU for the gold version and 1035.8 nm/RIU for the silver one, which is much better than many existing on-chip SPR devices. The assessment includes looking at transmission, reflection, and quality factors. This biosensor has great potential for detecting various biomolecules, such as markers for dengue and malaria, glucose levels, and blood electrolytes. It's set to be a low-cost, high-sensitivity option for diagnostics, especially in places with limited resources.

5.3 Recent advancements and future prospects

In future these structures have the capacity for performing bio-sensing platforms which are not only compact and cost effective but also highly adaptable for multiple analyte detection. Further development including integration with microfluidics and wireless data transmission might lead to novel devices that may be portable, wearable or implantable for continuous health monitoring. The ability to detect hemoglobin, mosquito-borne diseases, glucose and electrolytes makes them particularly suitable for point-of-care diagnosis applications, especially in resource-limited conditions. Besides, the novel application of Bismuth Selenide opens up new opportunities in 2D materials research and the potential expansion of detection range into infrared and terahertz directions, thus increasing the scope of biomedical and environmental applications.

5.4 Key challenges and research directions

Although the constructed MIM-based SPR biosensors have shown good results, a number of difficulties are still unsolved. The main challenging issue among others is the need to make very regular nanohole and grating structures, for which complex and costly lithographic techniques are required. One more particularly important problem period is ensuring material compatibility and long-term stability, especially when introducing totally new types like Bismuth Selenide, which in other words means the ability to keep a steady structure and optical properties. The third problem is that during the multi-analyte detection, resonance signals from different targets can be overlapped, increasing the complexity of data interpretation and rendering the detection process impossible without highly specialized signal processing tools. Moreover, the difficulty of moving from lab-scale prototypes to mass producing such sensors is a result of the fact that reproducing the sensor design on a large scale is one of the hard parts of the process. The process of enlarging the sensor structure to a centimeter length will lose the resolution of the sensor in detecting certain chemicals and eventually, the commercial product will be useless. The issue of integrating the biosensors with the laboratory chip sizes to the wafer style product becomes shining inversely in an application that calls for the product to be reduced, large-scale infrastructure projects need to be minimized not only the biotechnology industry but also in other fields.

Looking forward, the next area of investigation in studies about the biosensors can be on the way to combine these biosensors with microfluidic systems that are able to perform handling of the sample in an automated way, and carry out the analysis in real time, thus, making them more useful for clinical and point-of-care applications. The use of artificial intelligence and machine learning can further aid in analyzing data of high complexity and different spectra enhancing more accuracy in multi-analyte detection. It is reasonable to think that the new materials' further study provides 2D ones that are excellent in optical electronic and plasmonic natures, which can be used to do more in the detection process, for example, through more wavelengths and lower detection limits. For the development of wearable or implantable sensors, there is still a need for the sensor size to be reduced in addition to making the sensors to be compatible with the environment of the human body. To sum up, proving that these devices can work outside their labs, in the real world, and that they get good results in the clinical setting is going to be a game-changer for the devices' footsteps toward the medical diagnostics that are just necessary.

References

[1] H. H. Nguyen, J. Park, S. Kang, and M. Kim, "Surface plasmon resonance: a versatile technique for biosensor applications," *Sensors,* vol. 15, no. 5, pp. 10481-10510, 2015.

[2] V. Naresh and N. Lee, "A review on biosensors and recent development of nanostructured materials-enabled biosensors," *Sensors,* vol. 21, no. 4, p. 1109, 2021.

[3] J. Homola, "Present and future of surface plasmon resonance biosensors," *Analytical and bioanalytical chemistry,* vol. 377, no. 3, pp. 528-539, 2003.

[4] H.-f. Chen, C.-H. Lin, C.-Y. Su, H.-P. Chen, and Y.-L. Chiang, "Surface plasmon resonance biotechnology for antimicrobial susceptibility test," *Chapter,* vol. 21, pp. 453-468, 2011.

[5] M. Piliarik and J. Homola, "Surface plasmon resonance (SPR) sensors: approaching their limits?," *Optics express,* vol. 17, no. 19, pp. 16505-16517, 2009.

[6] R. Al Mahmud, R. Sagor, and M. Khan, "Surface plasmon refractive index biosensors: A review of optical fiber, multilayer 2D material and gratings, and MIM configurations," *Optics & Laser Technology,* vol. 159, p. 108939, 2023.

[7] J. Homola, "Surface plasmon resonance sensors for detection of chemical and biological species," *Chemical reviews,* vol. 108, no. 2, pp. 462-493, 2008.

[8] A. D. McFarland and R. P. Van Duyne, "Single silver nanoparticles as real-time optical sensors with zeptomole sensitivity," *Nano letters,* vol. 3, no. 8, pp. 1057-1062, 2003.

[9] S. Nath, "Advancements in food quality monitoring: integrating biosensors for precision detection," *Sustainable Food Technology,* 2024.

[10] A. Haleem, M. Javaid, R. P. Singh, R. Suman, and S. Rab, "Biosensors applications in medical field: A brief review," *Sensors International,* vol. 2, p. 100100, 2021.

[11] S. G. J. J. D. Joannopoulos, J. N. Winn, and R. D. Meade, "Photonic Crystals: Molding the Flow of Light," vol. 2nd ed., no. Princeton, NJ, USA: Princeton Univ. Press, 2008., 2008.

[12] P. Russell, "Photonic crystal fibers," *science,* vol. 299, no. 5605, pp. 358-362, 2003.

[13] S. G. Johnson and J. Joannopoulos, "Three-dimensionally periodic dielectric layered structure with omnidirectional photonic band gap," *Applied Physics Letters,* vol. 77, no. 22, pp. 3490-3492, 2000.

[14] J. Bravo-Abad, A. Rodriguez, P. Bermel, S. G. Johnson, J. D. Joannopoulos, and M. Soljačić, "Enhanced nonlinear optics in photonic-crystal microcavities," *Optics express,* vol. 15, no. 24, pp. 16161-16176, 2007.

[15] D. Gowdhami, V. Balaji, M. Murugan, S. Robinson, and G. Hegde, "Photonic crystal based biosensors: An overview," *ISSS Journal of Micro and Smart Systems,* vol. 11, no. 1, pp. 147-167, 2022.

[16] M. Loncar, D. Nedeljkovic, T. Doll, J. Vuckovic, A. Scherer, and T. P. Pearsall, "Waveguiding in planar photonic crystals," in *Silicon-based and Hybrid Optoelectronics III*, 2001, vol. 4293: SPIE, pp. 94-99.

[17] J. Homola, S. S. Yee, and G. Gauglitz, "Surface plasmon resonance sensors," *Sensors and actuators B: Chemical,* vol. 54, no. 1-2, pp. 3-15, 1999.

[18] T. A. Birks, J. C. Knight, and P. S. J. Russell, "Endlessly single-mode photonic crystal fiber," *Optics letters,* vol. 22, no. 13, pp. 961-963, 1997.

[19] A. A. Rifat, M. R. Hasan, R. Ahmed, and H. Butt, "Photonic crystal fiber-based plasmonic biosensor with external sensing approach," *Journal of Nanophotonics,* vol. 12, no. 1, pp. 012503-012503, 2018.

[20] D. Gao, C. Guan, Y. Wen, X. Zhong, and L. Yuan, "Multi-hole fiber based surface plasmon resonance sensor operated at near-infrared wavelengths," *Optics Communications,* vol. 313, pp. 94-98, 2014.

[21] M. A. Butt, N. L. Kazanskiy, and S. N. Khonina, "Metal-Insulator-Metal Waveguide Plasmonic Sensor System for Refractive Index Sensing Applications," *Advanced Photonics Research,* vol. 4, no. 7, p. 2300079, 2023.

[22] N. Tasnim and A. S. Mohsin, "Tunable MIM-Grating Based SPR Biosensor Using Metal-Bismuth Selenide (Bi2Se3)-Silicon Nitride (Si3N4) for Dengue, Malaria, Glucose, and Electrolyte Detection with Enhanced Sensitivity," *Physica Scripta,* 2025.

[23] M. A. Butt, "Plasmonic sensors based on a metal–insulator–metal waveguide—what do we know so far?," *Sensors,* vol. 24, no. 22, p. 7158, 2024.

[24] A. K. Goyal, "Design analysis of one-dimensional photonic crystal based structure for hemoglobin concentration measurement," *Progress In Electromagnetics Research M,* vol. 97, pp. 77-86, 2020.

[25] S. Kumar, A. Yadav, and B. A. Malomed, "Bimetal thin film, semiconductors, and 2D nanomaterials in SPR biosensors: an approach to enhanced urine glucose sensing," *IEEE Transactions on NanoBioscience,* vol. 23, no. 2, pp. 336-343, 2024.

[26] S. Sahu, N. Mudgal, A. Agrawal, and G. Singh, "Detection of Biomolecules and Glucose Concentration in Blood Using a Subwavelength Grating Optical Biosensor," *Journal of Sensors,* vol. 2023, no. 1, p. 5533918, 2023.

[27] M.-Y. Kim, S. H. Jee, J. E. Yun, S. J. Baek, and D.-C. Lee, "Hemoglobin concentration and risk of cardiovascular disease in Korean men and women-the Korean heart study," *Journal of Korean medical science,* vol. 28, no. 9, p. 1316, 2013.

[28] Y. Liu, S. Lu, Z. Zhang, Z. Yang, X. Cui, and G. Liu, "Printable biosensors towards next-generation point-of-care testing: paper substrate as an example," *Lab on a Chip,* vol. 23, no. 15, pp. 3328-3352, 2023.

[29] R. Zafar, S. Nawaz, G. Singh, A. d'Alessandro, and M. Salim, "Plasmonics-based refractive index sensor for detection of hemoglobin concentration," *IEEE Sensors Journal,* vol. 18, no. 11, pp. 4372-4377, 2018.

[30] A. Yadav, A. Kumar, P. Sharan, and M. Mishra, "Highly sensitive bimetallic-metal nitride SPR biosensor for urine glucose detection," *IEEE Transactions on NanoBioscience,* vol. 22, no. 4, pp. 897-903, 2023.

[31] S. Farhadi, A. Farmani, and A. Hamidi, "Figure of merit enhancement of surface plasmon resonance biosensor based on Talbot effect," *Optical and Quantum Electronics,* vol. 53, no. 9, p. 518, 2021.

[32] G. A. Lopez, M.-C. Estevez, M. Soler, and L. M. Lechuga, "Recent advances in nanoplasmonic biosensors: applications and lab-on-a-chip integration," *Nanophotonics,* vol. 6, no. 1, pp. 123-136, 2017.

[33] Y. Seo, S. Jeong, J. Lee, H. S. Choi, J. Kim, and H. Lee, "Innovations in biomedical nanoengineering: nanowell array biosensor," *Nano Convergence,* vol. 5, no. 1, p. 9, 2018.

[34] Z. Wang *et al.*, "An ultrasensitive plasmonic sensor based on 2D ferroelectric Bi2O2Se," *Small,* vol. 19, no. 45, p. 2303026, 2023.

[35] P. P. A. Suthanthiraraj and A. K. Sen, "Localized surface plasmon resonance (LSPR) biosensor based on thermally annealed silver nanostructures with on-chip blood-plasma separation for the detection of dengue non-structural protein NS1 antigen," *Biosensors and Bioelectronics,* vol. 132, pp. 38-46, 2019.

[36] C. Huang, K. Bonroy, G. Reekman, K. Verstreken, L. Lagae, and G. Borghs, "An on-chip localized surface plasmon resonance-based biosensor for label-free monitoring of antigen–antibody reaction," *Microelectronic Engineering,* vol. 86, no. 12, pp. 2437-2441, 2009.

[37] S. Raga, S. K. Gowre, and H. Miyan, "A 2D GaAs-Based Photonic Crystal Biosensor for Malaria Detection," *International Journal of Engineering & Technology Innovation,* vol. 13, no. 4, 2023.

[38] X. Mao and M. Cada, "Optical surface plasmon in semiconductors," in *Integrated Photonics Research, Silicon and Nanophotonics*, 2013: Optica Publishing Group, p. IM1B. 4.

[39] H. Shafiee *et al.*, "Nanostructured optical photonic crystal biosensor for HIV viral load measurement," *Scientific reports,* vol. 4, no. 1, p. 4116, 2014.

[40] P. Sharma, S. K. Roy, and P. Sharan, "Design and simulation of photonic crystal based biosensor for detection of different blood components," in *2014 IEEE Region 10 Symposium*, 2014: IEEE, pp. 171-176.

[41] L. J. Mendoza Herrera, D. M. Arboleda, D. C. Schinca, and L. B. Scaffardi, "Determination of plasma frequency, damping constant, and size distribution from the complex dielectric function of noble metal nanoparticles," *Journal of Applied Physics,* vol. 116, no. 23, 2014.

[42] S. K. Chamoli, S. C. Singh, and C. Guo, "Design of extremely sensitive refractive index sensors in infrared for blood glucose detection," *IEEE Sensors Journal,* vol. 20, no. 9, pp. 4628-4634, 2020.

[43] N. Ghosh, P. Buddhiwant, A. Uppal, S. Majumder, H. Patel, and P. Gupta, "Simultaneous determination of size and refractive index of red blood cells by light scattering measurements," *Applied physics letters,* vol. 88, no. 8, 2006.

[44] X. Liang, A. Liu, C. Lim, T. Ayi, and P. Yap, "Determining refractive index of single living cell using an integrated microchip," *Sensors and Actuators A: Physical,* vol. 133, no. 2, pp. 349-354, 2007.

[45] N. Lue *et al.*, "Live cell refractometry using Hilbert phase microscopy and confocal reflectance microscopy," *The Journal of Physical Chemistry A,* vol. 113, no. 47, pp. 13327-13330, 2009.

[46] W. Choi *et al.*, "Tomographic phase microscopy," *Nature methods,* vol. 4, no. 9, pp. 717-719, 2007.

[47] K. G. Phillips, S. L. Jacques, and O. J. McCarty, "Measurement of Single Cell Refractive Index, Dry Mass, Volume, and Density<? format?> Using a Transillumination Microscope," *Physical review letters,* vol. 109, no. 11, p. 118105, 2012.

[48] A. S. Mohsin and M. B. Salim, "Probing the intracellular refractive index and molecular interaction of gold nanoparticles in HeLa cells using single particle spectroscopy," *International journal of nanomedicine,* pp. 6019-6028, 2018.

[49] O. Zhernovaya, O. Sydoruk, V. Tuchin, and A. Douplik, "The refractive index of human hemoglobin in the visible range," *Physics in Medicine & Biology,* vol. 56, no. 13, p. 4013, 2011.

[50] M. Friebel and M. Meinke, "Determination of the complex refractive index of highly concentrated hemoglobin solutions using transmittance and reflectance measurements," *Journal of Biomedical Optics,* vol. 10, no. 6, pp. 064019-064019-5, 2005.

[51] A. K. Ajad, M. J. Islam, M. R. Kaysir, and J. Atai, "Highly sensitive bio sensor based on WGM ring resonator for hemoglobin detection in blood samples," *Optik,* vol. 226, p. 166009, 2021.

[52] C. H. Chu *et al.*, "Enhanced optical sensing with metal-insulator-metal nanohole arrays integrated with silver nanoparticles," *Results in Physics,* vol. 55, p. 107203, 2023.

[53] V. Faramarzi, V. Ahmadi, F. Ghane Golmohamadi, and B. Fotouhi, "A biosensor based on plasmonic wave excitation with diffractive grating structure," *Scientia Iranica,* vol. 24, no. 6, pp. 3441-3447, 2017.

[54] A. S. Mohsin and M. B. Salim, "Probing the plasmon coupling, quantum yield, and effects of tip geometry of gold nanoparticle using analytical models and FDTD simulation," *IEEE Photonics Journal,* vol. 10, no. 3, pp. 1-10, 2018.

[55] S. Sahu, J. Ali, P. P. Yupapin, and G. Singh, "Optical biosensor based on a cladding modulated grating waveguide," *Optik,* vol. 166, pp. 103-109, 2018.

[56] Y.-S. Peng, B. Xu, X.-L. Ye, J.-B. Niu, R. Jia, and Z.-G. Wang, "Fabrication of high quality two-dimensional photonic crystal mask layer patterns," *Optical and quantum electronics,* vol. 41, no. 3, p. 151, 2009.

[57] H. J. El-Khozondar, P. Mahalakshmi, R. J. El-Khozondar, N. Ramanujam, I. Amiri, and P. Yupapin, "Design of one dimensional refractive index sensor using ternary photonic crystal waveguide for plasma blood samples applications," *Physica E: Low-dimensional Systems and Nanostructures,* vol. 111, pp. 29-36, 2019.

[58] H. Farmani, A. Farmani, and Z. Biglari, "A label-free graphene-based nanosensor using surface plasmon resonance for biomaterials detection," *Physica E: Low-dimensional systems and Nanostructures,* vol. 116, p. 113730, 2020.

[59] H. Heidarzadeh, "Analysis and simulation of a plasmonic biosensor for hemoglobin concentration detection using noble metal nano-particles resonances," *Optics Communications,* vol. 459, p. 124940, 2020.

[60] S. Edappadikkunnummal, R. Chembra Vasudevan, S. Dinesh, S. Thomas, N. R. Desai, and S. Kaniyarakkal, "Detection of hemoglobin concentration based on defective one-dimensional photonic crystals," in *Photonics*, 2022, vol. 9, no. 9: MDPI, p. 660.

[61] N. Tasnim and A. S. Mohsin, "Nanohole array integrated metal insulator metal (MIM) based structure employing dual mode SPR sensor for detection of Hemoglobin (Hb) in blood," *Heliyon,* vol. 10, no. 12, 2024.

[62] L. B. Akcher, A. S. Mohsin, and M. A. Haque, "Study and simulation of MIM grating-based refractive index sensor for the detection of haemoglobin (Hb) in blood samples," *Plasmonics,* pp. 1-8, 2024.

[63] A. Boltasseva, "Plasmonic components fabrication via nanoimprint," *Journal of Optics A: Pure and Applied Optics,* vol. 11, no. 11, p. 114001, 2009.

[64] W. K. Jung and K. M. Byun, "Fabrication of nanoscale plasmonic structures and their applications to photonic devices and biosensors," *Biomedical Engineering Letters,* vol. 1, pp. 153-162, 2011.

[65] L. Gutierrez-Rivera, R. Peters, S. Dew, and M. Stepanova, "Surface-enhanced Raman spectroscopy detection of protein-ligand binding using D-glucose and glucose binding protein on nanostructured plasmonic substrates," *AIMS Materials Science,* vol. 4, no. 2, pp. 522-539, 2017.

[66] M. Radtke, R. Nelz, A. Slablab, and E. Neu, "Reliable nanofabrication of single-crystal diamond photonic nanostructures for nanoscale sensing," *Micromachines,* vol. 10, no. 11, p. 718, 2019.

[67] J. Li *et al.*, "Biocatalysis-induced formation of BiOBr/Bi2S3 semiconductor heterostructures: A highly efficient strategy for establishing sensitive photoelectrochemical sensing system for organophosphorus pesticide detection," *Sensors and Actuators B: Chemical,* vol. 331, p. 129451, 2021.

[68] R. A. Ulwali, H. K. Abbas, A. J. Karam, A. A. Al-Zuky, M. F. H. Al-Kadhemy, and A. H. Al-Saleh, "Surface Plasmon Resonance (SPR) Simulation of a Gold-Bismuth Bi-layer Gas Sensor," *Iraqi Journal of Science,* pp. 3402-3411, 2022.

[69] L. Novotny and B. Hecht, *Principles of nano-optics*. Cambridge university press, 2012.

[70] N. J. Halas, S. Lal, W.-S. Chang, S. Link, and P. Nordlander, "Plasmons in strongly coupled metallic nanostructures," *Chemical reviews,* vol. 111, no. 6, pp. 3913-3961, 2011.

[71] N. Mudgal, A. Saharia, K. K. Choure, A. Agarwal, and G. Singh, "Sensitivity enhancement with anti-reflection coating of silicon nitride (Si 3 N 4) layer in silver-based surface plasmon resonance (SPR) sensor for sensing of DNA hybridization," *Applied Physics A,* vol. 126, pp. 1-8, 2020.

[72] D. Kohler *et al.*, "Biophotonic sensors with integrated Si3N4-organic hybrid (SiNOH) lasers for point-of-care diagnostics," *Light: Science & Applications,* vol. 10, no. 1, p. 64, 2021.

[73] R. M. Rowan-Robinson *et al.*, "Thickness dependent enhancement of the polar Kerr rotation in Co magnetoplasmonic nanostructures," *AIP Advances,* vol. 9, no. 2, 2019.

[74] P. Sarapukdee, D. Schulz, and S. Palzer, "Grating Structures for Silver-Based Surface Plasmon Resonance Sensors with Adjustable Excitation Angle," *Sensors,* vol. 24, no. 14, p. 4538, 2024.

[75] J. Ehiabhili, R. Prabhu, and S. Kannan, "Highly sensitive D-SPR sensors with optimized metallic thin films for bio-analyte detection," in *Photonics*, 2024, vol. 11, no. 8: MDPI, p. 764.

[76] W. Organizatio, "Dengue and severe dengue," 2024.

[77] R. Rahad *et al.*, "A polarization independent highly sensitive metasurface-based biosensor for lab-on-chip applications," *Measurement,* vol. 231, p. 114652, 2024.

[78] D. A. Muller, A. C. Depelsenaire, and P. R. Young, "Clinical and laboratory diagnosis of dengue virus infection," *The Journal of infectious diseases,* vol. 215, no. suppl_2, pp. S89-S95, 2017.

[79] N. Djeffal, S. Bendib, and A. Hedir, "A dengue virus detection using biosensor-based two-dimensional photonic crystal ring resonator," in *Photonics*, 2025, vol. 12, no. 5: MDPI, p. 514.

[80] N. Tangpukdee, C. Duangdee, P. Wilairatana, and S. Krudsood, "Malaria diagnosis: a brief review," *The Korean journal of parasitology,* vol. 47, no. 2, p. 93, 2009.

[81] M. A. Agnero *et al.*, "Malaria-infected red blood cell analysis through optical and biochemical parameters using the transport of intensity equation and the microscope's optical properties," *Sensors,* vol. 19, no. 14, p. 3045, 2019.

[82] M. Meinke, G. Müller, J. Helfmann, and M. Friebel, "Optical properties of platelets and blood plasma and their influence on the optical behavior of whole blood in the visible to near infrared wavelength range," *Journal of biomedical optics,* vol. 12, no. 1, pp. 014024-014024-9, 2007.

[83] N. Haider, M. N. Hasan, J. Onyango, and M. Asaduzzaman, "Global landmark: 2023 marks the worst year for dengue cases with millions infected and thousands of deaths reported," *IJID regions,* vol. 13, p. 100459, 2024.

[84] W. H. Organization, *World malaria report 2023*. World Health Organization, 2023.

[85] T. Tougan *et al.*, "The malaria parasite Plasmodium falciparum in red blood cells selectively takes up serum proteins that affect host pathogenicity," *Malaria journal,* vol. 19, pp. 1-13, 2020.

[86] C. Garcia, "Calcium homeostasis and signaling in the blood-stage malaria parasite," *Parasitology Today,* vol. 15, no. 12, pp. 488-491, 1999.

[87] J. E. Hall and M. E. Hall, *Guyton and Hall Textbook of Medical Physiology E-Book: Guyton and Hall Textbook of Medical Physiology E-Book*. Elsevier Health Sciences, 2020.

[88] M. F. Hassan, R. H. Sagor, M. R. Amin, M. R. Islam, and M. S. Alam, "Point of care detection of blood electrolytes and glucose utilizing nano-dot enhanced plasmonic biosensor," *IEEE Sensors Journal,* vol. 21, no. 16, pp. 17749-17757, 2021.

[89] C.-Y. Tan and Y.-X. Huang, "Dependence of refractive index on concentration and temperature in electrolyte solution, polar solution, nonpolar solution, and protein solution," *Journal of Chemical & Engineering Data,* vol. 60, no. 10, pp. 2827-2833, 2015.

[90] B. H. Kumar, P. Srikanth, and A. Vaibhav, "A novel computation method for detection of Malaria in RBC using Photonic biosensor," *International journal of information technology,* vol. 13, no. 5, pp. 2053-2058, 2021.

[91] S. K. Saini and S. K. Awasthi, "Sensing and detection capabilities of one-dimensional defective photonic crystal suitable for malaria infection diagnosis from preliminary to advanced stage: theoretical study," *Crystals,* vol. 13, no. 1, p. 128, 2023.

[92] B. Mohapatra, A. S. Khan, D. Dash, and M. R. Ansari, "Design of biosensor using 1D photonic crystal for dengue virus detection," in *2022 4th International Conference on Advances in Computing, Communication Control and Networking (ICAC3N)*, 2022: IEEE, pp. 1667-1670.

[93] F. Baraty and S. Hamedi, "Design of a 2D photonic crystal biosensor using X-shape ring resonator based on Graphene Oxide (GO) for detection of blood components," *Journal of Electromagnetic Waves and Applications,* vol. 36, no. 17, pp. 2401-2418, 2022.